Shedding light on blue-green photosynthesis: A wavelength-dependent mathematical model of photosynthesis in *Synechocystis* sp. PCC 6803

Tobias Pfennig[1,2,*], Elena Kullmann[1], Tomáš Zavřel[3], Andreas Nakielski[1,4], Oliver Ebenhöh[2,5], Jan Červený[3], Gábor Bernát[6], and Anna Matuszyńska[1,2]

[1]Computational Life Science, Department of Biology, RWTH Aachen University, 52074 Aachen, Germany
[2]Cluster of Excellence on Plant Sciences, Heinrich Heine University (HHU) Düsseldorf, Germany
[3]Department of Adaptive Biotechnologies, Global Change Research Institute, Czech Academy of Sciences, Brno, Czechia
[4]Institute for Synthetic Microbiology, HHU Düsseldorf, Düsseldorf, Germany
[5]Institute of Theoretical and Quantitative Biology, HHU Düsseldorf, Düsseldorf, Germany
[6]HUN-REN Balaton Limnological Research Institute, Tihany, Hungary
[*]Corresponding authors
E-mail: tobias.pfennig@rwth-aachen.de (TP) & anna.matuszynska@cpbl.rwth-aachen.de (AM)

Abstract

Cyanobacteria hold great potential to revolutionize conventional industries and farming practices with their light-driven chemical production. To fully exploit their photosynthetic capacity and enhance product yield, it is crucial to investigate their intricate interplay with the environment including the light intensity and spectrum. Mathematical models provide valuable insights for optimizing strategies in this pursuit. In this study, we present an ordinary differential equation-based model for the cyanobacterium *Synechocystis* sp. PCC 6803 to assess its performance under various light sources, including monochromatic light. Our model can reproduce a variety of physiologically measured quantities, e.g. experimentally reported partitioning of electrons through four main pathways, O_2 evolution, and the rate of carbon fixation for ambient and saturated CO_2. By capturing the interactions between different components of a photosynthetic system, our model helps in understanding the underlying mechanisms driving system behavior. Our model qualitatively reproduces fluorescence emitted under various light regimes, replicating Pulse-amplitude modulation (PAM) fluorometry experiments with saturating pulses. Using our model, we test four hypothesized mechanisms of cyanobacterial state transitions. Moreover, we evaluate metabolic control for biotechnological production under diverse light colors and irradiances. By offering a comprehensive computational model of cyanobacterial photosynthesis, our work enhances the basic understanding of light-dependent cyanobacterial behavior and sets the first wavelength-dependent framework to systematically test their producing capacity for biocatalysis.

Keywords: biocatalysis | cyanobacteria | electron transport | light spectrum | state transitions.

Introduction

Cyanobacteria are responsible for a quarter of global carbon fixation [1]. They are, in fact, the originators of oxygenic photosynthesis, later transferring this capability to other organisms via endosymbiosis [2]. Despite their relative simplicity in cellular structure, the cyanobacterial photosynthetic machinery is a highly sophisticated system that shows significant differences from their plastidic relatives [3]. Recently, they have emerged as a powerful resource for research and biotechnology due to their unique combination of beneficial traits and photosynthetic capabilities [4]. In the quest for environmentally friendly alternatives to fossil fuels and sugar-based production, cyanobacteria stand out as promising candidates due to their ability to convert sunlight and CO_2 into valuable products, their minimal growth requirements, and their adaptability to diverse environments. Their metabolic versatility allows for

producing a wide range of biofuels, chemicals, and raw materials. Besides biomass [5], the cells can be harvested for a variety of primary and secondary metabolites, such as sugars and alcohols [6, 7], chlorophyll and carotenoids [4], (poly)peptides and human vitamins [8], and terpenoids [9]. In particular, strains of the model cyanobacteria *Synechocystis* sp. PCC 6803 and *Synechococcus elongatus* PCC 7942, are highly attractive platform organisms for the phototrophic production of e.g. isoprene, squalene, valencene, cycloartenol, lupeol or bisabolene [9]. Leveraging the cells' natural capabilities, isolation of molecular hydrogen [10] and reduced nitrogen [4] is also possible, with uses in energy and agronomic sectors. Furthermore, there have been attempts to use cyanobacteria for bioelectricity production [7, 11] or, inversely, to overcome cellular limitations by fuelling cyanobacteria with induced electrical currents [12].

Modifying metabolism for biotechnological purposes involves overcoming natural regulations and inhibitory mechanisms, disrupting the metabolic network's balance. However, balance is crucial for a proper photosynthetic function [13] and, thus, the viability of cyanobacteria for biotechnology. Therefore, a comprehensive understanding of primary and secondary metabolism is essential for effective and compatible modifications. Mathematical models integrate and condense current knowledge to identify significant parts and interactions, enabling the simulation of the effect of various external factors and internal modifications [14, 15]. They can also provide a platform to test new hypotheses. Numerous plant models of primary metabolism helped to identify the most favorable environmental conditions, nutrient compositions, and genetic modifications to maximize the desired outputs [16, 15]. Despite the evolutionary connection between cyanobacteria and plants, the structural and kinetic differences between cyanobacteria and plants (e.g., competition for electrons due to respiration [17], phycobilisomes (PBSs) as cyanobacterial light-harvesting antennae, photoprotection mediated by Orange Carotenoid Protein (OCP), existence of Carbon Concentrating Mechanism (CCM)) prevent the use of established plant-based models for photosynthesis [3, 17, 18, 19, 20, 21]. Even standard experimental methods developed for plants for non-invasive probing of photosynthesis using spectrometric techniques, such as Pulse Amplitude Modulation (PAM) fluorometry and the Saturation Pulse method (PAM-SP)[22], may require either adaptation or change in the interpretation of the measurements when applied to cyanobacteria [3, 23, 24]. In PAM fluorometry, a modulated light source is used to excite the chlorophyll molecules [22]. The emitted fluorescence is then measured, and various parameters derived from this fluorescence signal can provide insights into the efficiency of photosynthesis, the health of the photosynthetic apparatus, and other aspects of plant physiology. Compared to plants and green algae, the measured fluorescence of cyanobacteria has contributions from PSII, PSI, and detached PBS resulting in distinct fluorescence behavior [3, 24, 25, 26].

Therefore, a mathematical model targeted specifically for cyanobacteria, and capable of simulating and interpreting their re-emitted fluorescence signal after various light modulations is needed to obtain a system perspective on their photosynthetic dynamics. Established cyanobacterial models often describe broad ecosystem behavior or specific cellular characteristics [27]. Worth mentioning here are constrained-based reconstructions of primary metabolic networks [28, 29, 30], as well as kinetic models, ranging from simple models of non-photochemical quenching [31] and fluorescence [26] to adapted plant models to study the dynamics of cyanobacterial photosynthesis [32] and models created to study proteome allocation as a function of growth rate [33]. However, none of these models provide a detailed, mechanistic description of oxygenic photosynthesis in *Synechocystis* sp. PCC 6803, including the dynamics of respiration and a mechanistic description of short-term acclimation mechanisms, which are highly sensitive to changes in light wavelengths.

With this work, we provide a detailed description of photosynthetic electron flow in cyanobacteria (as summarized in Fig. 1a), parameterized to experimental data, including measurements collected under monochromatic light, in *Synechocystis* sp. PCC 6803, a unicellular freshwater cyanobacterium. Light is a critical resource for photosynthetic prokaryotes, which defines their ecological niche and heavily affects cell physiology [24, 34, 35]. Significantly, beyond its intensity, the light spectrum plays a crucial role in exerting physiological control. For example, growth under various monochromatic light sources led to large differences in cyanobacterial growth rate, cell composition, and photosynthetic parameters [36]. Blue light strongly inhibits growth and can cause cell damage by disrupting the excitation balance of photosystems [29, 37, 38], resulting from the varying absorption properties of their pigments [38]. To react to changes in illumination, the cell is able to undergo both short and long-term adaptations. Over time, cells adjust their pigment content (in a process called chromatic acclimation), and the ratio of photosystems to optimize performance [35, 24]. In the short term, processes like OCP-related Non-Photochemical Quenching (NPQ) [39, 40] or state transitions [41] help them adapt, though precise mechanisms of the latter are not yet fully elucidated [3, 42]. While the scientific community agrees

that the PQ redox state triggers state transitions, multiple underlying mechanisms have been proposed without a current consensus. Our model uses therefore both light intensity and light wavelengths as input, allowing the simulation of any combination of light sources and adaptation to the specific growth conditions. Readouts include all intermediate metabolites and carriers, most importantly ATP and NADPH, fluxes through several electron pathways: Linear Electron Transport (LET), Respiratory Electron Transport (RET), Cyclic Electron Transport (CET) and Alternate Electron Transport (AEF)), reaction rates, such as carbon fixation and water splitting, and the cell's emitted fluorescence as measured by PAM. We perform Metabolic Control Analysis (MCA) [43, 44, 45] of the network in different light conditions, showing that the reactions which determine the rate of CBB flux shift from photosynthetic source reactions to sink reactions within the CBB as light intensity increases. By harnessing the power of mathematical modelling, we seek to provide a quantitative framework to test further hypothesis on the photosynthetic mechanisms in cyanobacteria and contribute to basic research on these organisms that eventually can lead to optimized cyanobacterial production and contribute to the advancement of green biotechnology.

Methods

Model description

We developed a dynamic, mathematical model of photosynthetic electron transport in *Synechocystis* sp. PCC 6803 (further *Synechocystis*) following a classical bottom-up development cycle. Our model consists of a system of 17 coupled Ordinary Differential Equations (ODEs), 27 reaction rates, and 95 parameters, including measured midpoint potentials, compound concentrations, absorption spectra, and physical constants (Table S3). By integrating the system over time, we can simulate the dynamic behavior of rates and concentrations of all reactions and reactants visualized on Fig. 1a and summarized in Table S2, including dynamic changes in the lumenal and cytoplasmic pH. We included a detailed description of four commonly distinguished electron transport pathways: LET, CET, RET, and AEF. Given the high similarity between the essential electron transport chain proteins of plants and cyanobacteria [3, 20], the photosystems were described using Quasi-Steady-State (QSS) approximation, as derived in our previous dynamic models of photosynthetic organisms [47, 48]. We followed a reductionist approach simplifying many downstream processes into lumped reactions. The lumped CBB, PR, and metabolic consumption reactions represented the main cellular energy sinks. Functions describing CBB and RuBisCO oxygenation (Oxy) contained multiple regulatory terms, including gas and metabolite concentrations (see SI). Although cyanobacteria CCM components include at least four modes of active inorganic carbon uptake [49], we have decided to represent the mechanism as a one lump reaction. By calculating the dissolved CO_2 concentration at the cellular pH and with an actively 1000-fold increased intracellular CO_2 gas pressure (see Supplement S1.12) we reflect the very efficient cyanobacterial concentrating mechanism. Unless stated otherwise, simulations were run under three assumptions: 25 °C temperature with 230 µmol L^{-1} dissolved O_2 and supplemented with 5 % CO_2. The pigment content and photosystems ratio were parametrized to a cell grown under ambient air with 25 µmol(photons) m^{-2} s^{-1} of 633 nm light. All rates and concentrations have been normalized to the chlorophyll content (4 mmol L^{-1}). The default initial metabolite concentrations were set to literature measurements (Table S1). Steady-state simulations were run for 1×10^6 s. For the steady-state simulations, we considered that the steady-state is reached if the Euclidean norm of relative concentration changes between the last two time steps did not exceed 1×10^{-6}. Because the regulatory processes, CBB redox activation, OCP activation, and state transitions, have slow rates of change, we compared their relative changes to a threshold of 1×10^{-8}.

Code implementation

The model has been developed in `Python` [50] using the modeling package `modelbase` [51] further exploring a highly modular approach to programming mathematical models. The model and scripts used to numerically integrate the system and to produce all figures from this manuscript, as well as analysis run during the peer review process are accessible at `https://github.com/Computational-Biology-Aachen/synechocystis-photosynthesis-2024`.

Model Parameterization

The model has been manually parameterized, integrating physiological data and dynamic observations from numerous groups (pH-ranges: [52], NADPH reduction: [53], O_2 change rates: [25], CO_2 consumption: [33], PQ reduction: [54], PC, PSI, and Fd redox-states: [55], PAM-behavior: [42], electron fluxes: [46], PAM fluorescence: [56]).

The model depends on 96 parameters (Table S3). 43 parameters, including pigment absorption

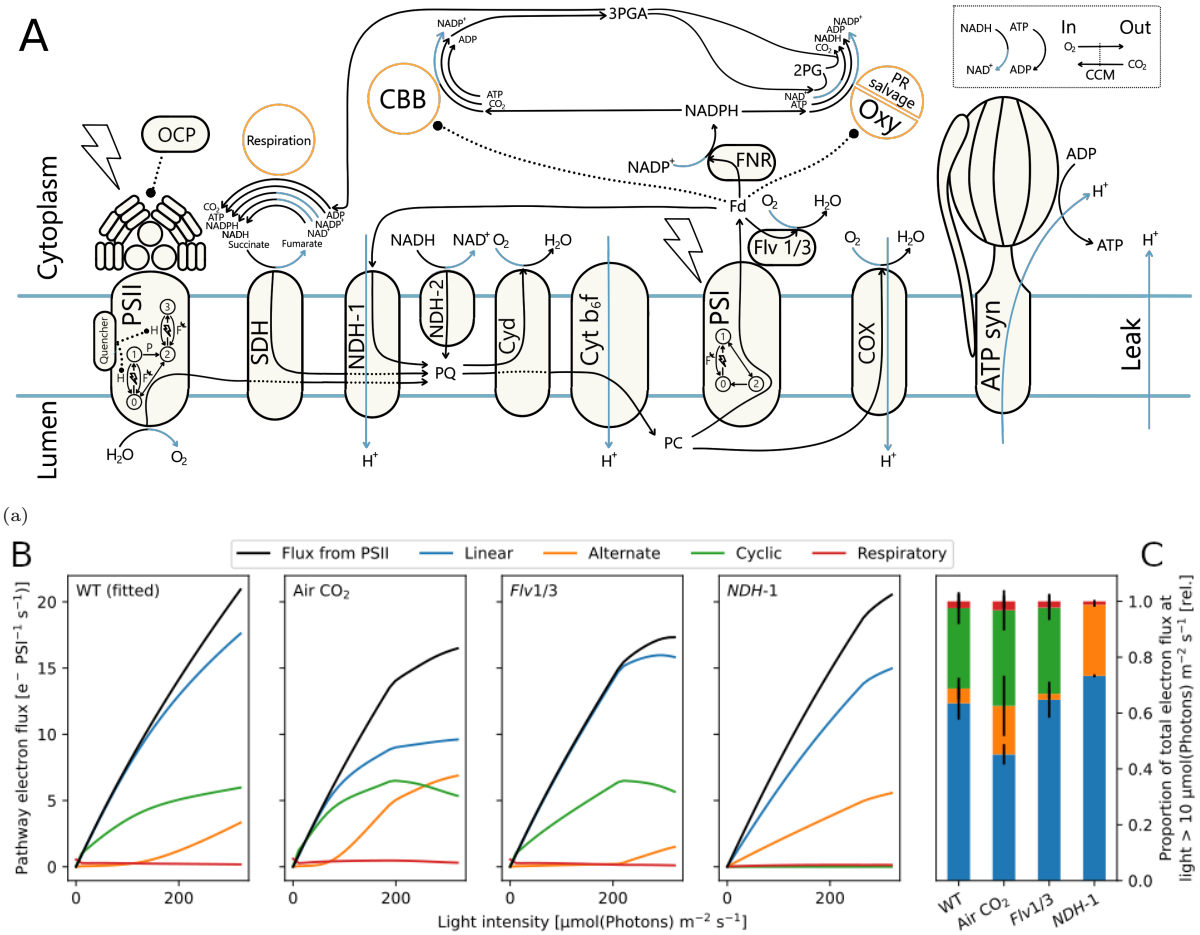

Fig. 1: **Computational model of the photosynthetic and respiratory chain allows simulating electron fluxes through main (linear), cyclic, alternate, and respiratory pathways in *Synechocystis* sp. PCC 6803. a)** Schematic representation of components and reactions included in the model of cyanobacterial photosynthesis. The model includes descriptions of four protein complexes (PSII, PSI, Cb_6f and ATP synthase), main electron carriers and reactions through them, enabling simulation of electron transfer through Linear Electron Transport (LET), Cyclic Electron Transport (CET), Respiratory Electron Transport (RET), and Alternate Electron Transport (AEF). With orange circles (Respiration, CBB, and photorespiratory salvage pathway (PR salvage)) we mark pathways represented in the model as lumped reactions. The top-right box shows gas exchange reactions (O_2 export and active CO_2 import) and metabolic ATP and NADH consumption. Electron and proton flows are colored black and blue, respectively. Regulatory effects, such as Fd-dependent CBB activity, are represented with dotted lines. The two photosystems are described using Quasi-Steady-State (QSS) approximation. For the analyzes we assume internal quencher as the state transition mechanism, as marked on PSII. Various scenarios of PBS attachment can be simulated, on the figure attached to PSII. **b)** Simulated steady-state electron flux through linear (blue), cyclic (green), alternate (flavodiiron+terminal oxidases, orange) and respiratory (red) electron pathways for light intensities between 10 µmol(photons) m^{-2} s^{-1} and 300 µmol(photons) m^{-2} s^{-1}. The model has been **parameterized** to yield approximately 15 electrons PSI^{-1} s^{-1} linear electron flow (blue) for a fraction of 60 % under saturating CO_2 conditions, as measured in wild type (WT) [46]. The model **predicts** flux distributions under sub-saturating air CO_2 level and for the flavodiiron (*Flv*1/3) and NAD(P)H Dehydrogenase-like complex 1 (NDH-1) knockout mutants. Each value represents a steady-state flux under continuous light exposure. Simulations were run using 670 nm light (Gaussian LED, $\sigma = 10$ nm). The barplot shows the mean flux distribution for light intensities over 10 µmol(photons) m^{-2} s^{-1}. Error bars show sd. Abbreviations: 2PG: 2-phosphoglycolate, 3PGA: 3-phosphoglycerate, ADP: Adenosine diphosphate, ATP: Adenosine triphosphate, ATPsynth: ATP synthase, CBB: Calvin-Benson-Bassham cycle, CCM: Carbon Concentrating Mechanism, COX(aa_3): Cytochrome c oxidase, Cyd(bd): Cytochrome bd quinol oxidase, Cyto b_6f: Cytochrome b_6f complex, FNR: Ferredoxin-$NADP^+$ Reductase, Fd: Ferredoxin, $NADP^+$: Nicotinamide adenine dinucleotide phosphate, NADPH: reduced Nicotinamide adenine dinucleotide phosphate, NAD^+: Nicotinamide adenine dinucleotide, NADH: reduced Nicotinamide adenine dinucleotide, NDH-2: NAD(P)H Dehydrogenase complex 2, OCP: Orange Carotenoid Protein, Oxy: RuBisCO oxygenation, PC: Plastocyanine, PQ: Plastoquinone, PR: Photorespiration, PSI: Photosystem I, PSII: Photosystem II, SDH: Succinate dehydrogenase

spectra, were taken directly from the literature, six parameters describe the experimental setup (light: intensity and spectrum, CO_2, O_2, concentration of cells, and temperature), and eight parameters describing photosystems concentrations and pigment composition were estimated from provided data [56]. The latter parameters were measured spectrophotometrically and through 77 K fluorescence, assuming a 10-times higher fluorescence yield of free PBS (compare [26]). PAM-SP fluorescence curves were used to fit seven fluorescence-related parameters, including quenching and OCP constants [56], and two parameters were fit to electron transport rate measurements [46]. Nine rate parameters were estimated from reported rates of the reaction itself or connected processes such as O_2 generation for respiration. To derive rate constants, we divided the determined rate by the assumed cellular substrate concentrations. Five parameters stemmed from simplifying assumptions regarding inhibition constants, the cytoplasmic salinity, and pH buffering. 16 further parameters were fitted to reproduce literature behavior such as cellular redox states or regulation of the CBB.

To avoid overfitting the parameters to a particular experimental set-up, we avoided using sophisticated fitting algorithms and instead proceeded with manual curation. At every step of model refinement we have been comparing visually how the change affects our simulated redox state, oxygen evolution, carbon fixation, and dynamics of implemented photoprotective mechanisms. A comprehensive list of all the model parameters utilized in this study, including values needed for unit conversion, is provided in Table S3 and Table S4 (state transition analysis separate, see below), ensuring transparency and reproducibility of our computational approach.

Reaction kinetics

Following the principle of parsimony, all reactions where no additional regulatory mechanism was known have been implemented with first-order Mass-Action (MA) kinetics. A reaction with substrates S_i and products P_j is defined as: $\sum n_i S_i \longleftrightarrow \sum m_j P_j \quad$ with $i, j \in \mathbb{N}$ where n_i and m_j are the stoichiometric coefficients of substrates and products, respectively. For each reaction, we calculated the Gibbs free energy ($\Delta_r G'$, see supplemental information) [47, 48]. Only reactions with $\Delta_r G'$ close to 0 under physiological conditions were described with reversible kinetics. Thus, we set reactions as irreversible except for ATP synthase, SDH, FNR, regulatory variables (e.g. CBB activation), and PSII and PSI internal processes.

To simplify higher order reversible MA equations [57], we first decompose the rate equation into separate kinetic and thermodynamic components (as done for Michaelis-Menten (MM) [58]) and then simplify only the kinetic part, leading to (see Equation S3 and S5):

$$v = \begin{cases} \text{if } \Delta_r G' < 0: & \overbrace{k^+ \cdot \prod c_{S_i}}^{\text{kinetic}} \cdot \overbrace{(1 - \exp(\Delta_r G'/RT))}^{\text{thermodynamic}} \\ \text{else:} & k^- \cdot \frac{\prod c_{P_j}}{K_{eq}} \cdot (\exp(-\Delta_r G'/RT) - 1) \end{cases} \tag{1}$$

with substrate concentrations c_S, product concentrations c_P, and $K_{eq} = \exp(-\Delta_r G'^0/RT)$. Here, we approximate $k \cdot \prod c_{S_i}^{n_i} \approx k^+ \cdot \prod c_{S_i}^{n_i} / \prod c_{S_i}^{n_i - 1}$ and $k \cdot \prod c_{P_j}^{m_j} \approx k^- \cdot \prod c_{P_j}^{m_j} / \prod c_{P_j}^{m_j - 1}$ which, for any $n_i > 1$ or $m_j > 1$, leads to $k^+ \neq k^-$ (see Equation S6). This necessitated parameterising k^+ and k^- separately. The reactions FNR and SDH, which were deemed reversible, used rate Equation 1 with the determination of $\Delta_r G'$ during simulation. We calculated electron pathway fluxes from the following involved reactions: LET (FNR), CET (NDH-1), respiration (SDH, NDH-2), and AEF (Cyd, COX, Flv) (see Equation S47).

Implementation of monochromatic and polychromatic light sources

To consider the influence of light spectrum on photosynthetic activity, our model takes light as input (I) with wavelengths (λ) in range between 400 and 700 nm. In this work we performed simulations using the solar spectrum, a fluorescent lamp, cold white LED, warm white LED, and "gaussian LEDs" simulated as Gauss curves with a set peak-wavelength and variance of 10 nm or 0.001 nm ("near monochromatic") [59] (see Fig. 3a & Fig. S11).

For calculation of absorbed light we further differentiate between the light absorbed by PSI, PSII, and PBS, based on their reported pigment composition [59] (Fig. 3a). We focused on four most abundant pigments: chlorophyll, beta-carotene, phycocyanin, and allophycocyanin, although the implementation allows for more complex composition. We assume that PBSs can be either free, in which case the excitation is lost, or attached to one of the photosystems to transfer their excitation energy. The respective fractions of PBS states were fixed to values from [56], except for simulations of state transition

mechanisms which required dynamic PBS behavior. We assumed pigment content and PBS-attachment as measured by Zavřel *et al.* [56], although different pigment composition can be provided as an input to the model. We calculate PSII excitation rate E_{PSII} (and E_{PSI} analogically) as:

$$E_{PSII} = P^{PSII} \cdot Q_{OCP} \cdot \text{simpson}(A \cdot \text{diag}(I)) \cdot lcf \tag{2}$$

where vector $P_{1\times4}$ denotes absorbed photons redistributed to either photosystem, accounting e.g. for their pigment composition, high PSI:PSII ratio and the PBS attachment; $Q_{OCP} = \text{diag}(1, 1, 1{-}OCP, 1{-}OCP)$ is a diagonal matrix with values set to one everywhere but at the contribution of PBS to reduce the excitation rate by light energy quenched due to OCP activity; $A_{p\times\lambda} = (a_{\lambda,p})$ contains each pigment p's-specific absorption spectra; "simpson" is a row-wise, numerical integral of the light absorbed by each considered pigment, calculated using the composite Simpson's rule (we used `scipy.integrate.simpson` function); $lcf = 0.5$ is the light conversion factor to estimate the amount of generated excitations, which was fitted to match the electron transfer rates of Theune *et al.* [46] (Fig. 1b). Importantly, we assume that despite the wavelength-dependent energy content, all photons result in equivalent excitation of photosystems with the extra energy being lost as heat [60, 61]. This implementation enabled us to simulate various light-adapted cells by updating the parameters corresponding to measured pigment composition and photosystem ratio. For simulations of PAM-SP, we further calculate the light encountered by a mean cell (I) for each wavelength according to an integrated Lambert-Beer function [62] accounting for the decreasing irradiance at various depths due to cellular absorption (see SI Equation S67).

Activation of photosystems

Following our previous approach [47], we modeled the photosystem's excitation and internal electron transport assuming that i) they are at Quasi-Steady-State (QSS), as they operate on a much faster time scale than other photosynthetic reactions, and ii) at every time point, photosystem II can be in one of four possible states, and PSI in three, relating pigment excitation with the charge separations at reaction centers (Fig. S1). The PSII excitation rate constant k_{LII} is calculated from E_{PSI} in Equation 2 (in µmol(photons) mg(chl)$^{-1}$) multiplied by the molar mass of chlorophyll M_{Chl} and normalized to PSII concentration:

$$k_{LII} = E_{PSI} \cdot M_{Chl} \cdot \frac{1}{c_{II}} \tag{3}$$

PSII was described with four (B_0 - B_3) and PSI with three states (Y_0 - Y_2) (see Fig. 1a and Fig. S1). The QSS models also consider the relaxation of excitations by fluorescence or heat emission (only PSII). We defined the PSII rate v_{PSII} as

$$v_{PSII} = 0.5 \cdot k_2 \cdot B_1 \tag{4}$$

since two $B_1 \rightarrow B_2$ reactions have to occur for a full PQ reduction.

Calculating the fluorescence signal

Based on the principle of PAM measurements, the model calculates fluorescence proportional to the gain in excited internal states of PSII and PSI when adding measuring light to the growth light. Additionally, we consider fluorescence of free PBS using their light absorption [26]. The default measuring light is set to 625 nm at 1 µmol(photons) m^{-2} s^{-1} throughout this manuscript.

PAM fluorometry measures the cellular fluorescence emitted in response to microsecond pulses of measuring light with a constant, low intensity. We built our model fluorescence function on the same principle. Measuring light pulses with irradiance I_{ML} are applied on top of the actinic light I, so cells experience a total irradiance of $I_{+ML} = I + I_{ML}$. We then recalculate the photosystems' QSS systems using I_{+ML}, resulting in the internal states B_0^{+ML} to B_3^{+ML} and Y_0^{+ML} to Y_2^{+ML}. We then define the PAM fluorescence as the increase in photosystem fluorescence reactions by the addition of measuring light (see Fig. S1):

$$F_{PSII} = k_F \cdot (B_1^{+ML} - B_1 + B_3^{+ML} - B_3) \tag{5}$$

$$F_{PSI} = k_{F1} \cdot (Y_1^{+ML} - Y_1) \tag{6}$$

Lastly, we make the simplifying assumption that PBS fluorescence only results from the fraction of uncoupled PBS f_{free}^{PBS} and is proportional to their absorption of I_{+ML}:

$$F_{PBS} = \text{simpson}_\lambda(p_{\lambda,PBS} \cdot \text{diag}(I_{+ML})) \tag{7}$$

Considering cyanobacterial optical properties of light-harvesting pigments, fluorescence measured at room temperature can originate from both photosystems and PBS [3]. There have been attempts to determine the fluorescence contributions of each component [26]. We assume that the three fluorescent species contribute differently to the fluorescence detected $> 650\,\mathrm{nm}$, e.g. because of differing emission spectra. Therefore, we include weighing factors when calculating the total recorded fluorescence in Equation 8, which were calculated in Fig. 2a fitting. We estimate the total measured fluorescence signal by calculating the weighted sum of PSI, PSII, and PBS fluorescence:

$$F = w_{PS1} \cdot F_{PS1} + w_{PS2} \cdot F_{PS2} + w_{PBS} \cdot F_{PBS}, \tag{8}$$

where weights w were manually fitted to reproduce the fluorescence dynamics under changing light conditions of the experiment displayed in Figure 3 (fitted values can be found in (Table S3) as `fluo_influence`).

Testing four possible mechanisms of state transitions

We intended to use the model to provide quantitative arguments for a possible mechanism of state transitions that is not yet fully elucidated. We have implemented and tested four proposed state transition mechanisms based on a recent review [42] (Fig. 4a.) We model the transition to state 2 depending on reduced PQ (PQ_{red}) and to state 1 on oxidized PQ (PQ_{ox}). We implemented the default PSII-quenching (used for simulations in Fig. 2a) using a constitutively active quenching reaction and a reverse reaction with Hill kinetics. The remaining state transition models were described with few reactions and using MA kinetics. A complete mathematical description of the implementations is available in the SI. For the analysis, we systematically varied the parameter sets of all implementations and compared the steady-state fluorescence and PQ redox state under different lighting conditions (actinic: 440 nm at $80\,\mu\mathrm{mol(photons)\,m^{-2}\,s^{-1}}$ or 633 nm at $50\,\mu\mathrm{mol(photons)\,m^{-2}\,s^{-1}}$; measuring: 625 nm at $1\,\mu\mathrm{mol(photons)\,m^{-2}\,s^{-1}}$) (parameters in Table S5).

Metabolic Control Analysis

Metabolic Control Analysis (MCA) is a quantitative framework to study how the control of metabolic pathways is distributed among individual enzymes or steps within those pathways. It quantifies the change in steady-state compound concentrations or reaction fluxes in response to perturbation of an examined reaction [43, 45]. We used the `modelbase.mca` function `get_response_coefficients_df` to perform MCA on our model. The function is using definitions proposed by [63, 43] and calculates the flux control coefficients ($C^{J_j}_{v_k}$) and concentration control coefficients ($C^{S_j}_{v_k}$) using formulas:

$$C^{J_j}_{v_k} = \frac{v_k}{J_j} \frac{\partial J_j / \partial p_k}{\partial v_k / \partial p_k}, \tag{9}$$

$$C^{S_j}_{v_i} = \frac{v_k}{S_j} \frac{\partial S_j / \partial p_k}{\partial v_k / \partial p_k}, \tag{10}$$

where J_j and S_j are respectively the steady-state fluxes and concentrations of the system, p_k is a kinetic parameter which affects directly only reaction k with the rate v_k (see [63, 43]). We approximated these formulas numerically using the central difference, varying the parameters by $\pm 1\%$. MCA has been repeated for various simulated irradiances (Fig. 3a). For systematic analysis of the effect of various light sources on the rate of carbon fixation, we calculated the absolute of the control coefficients and show the mean of the following sets of model reactions: Photosystems (PSI, PSII), light-driven (PSI, PSII, Cytochrome b_6f complex, NDH-1, FNR), alternate (Flv, Cytochrome bd quinol oxidase (Cyd), Cytochrome c oxidase), and respiration (lumped respiration, Succinate Dehydrogenase, NDH-2).

Analysis of the production capacity

Exploring highly modular structure of the model, for determining the production potential of a biotechnological compound, we simply added an irreversible model reaction consuming ATP, NADPH, and Fd in the required ratio. We assume optimality of carbon provision by the CBB and, thus, set its rate to zero and add the energy equivalent cost of carbon fixation to the cost of the biotechnological compound. The sink reaction was described using simplified MA kinetics with a rate constant sufficient to prevent substrate accumulation under any light intensity (here set to 5000 (unit depending on the

order of the reaction) for every sink). Additionally, we added MA reactions draining ATP and NADPH with a very high rate constant ($10\,000\,s^{-1}$) if their pools became filled over 95 % to avoid sink limitation by either compound.

Results

We present the first kinetic model of photosynthesis developed for cyanobacteria that can simulate its dynamics for various light intensities and spectra. It is developed based on well-understood principles from physics, chemistry, and physiology, and is used as a framework for systematic analysis of the impact of light on photosynthetic dynamics. Our analysis focuses on several key aspects: the redox state of electron carriers, carbon fixation rates in ambient air, reproduction of fluorescence dynamics under changing light conditions, and the electron flow through main pathways (LET, CET, AEF) under different conditions. We used O_2 measurements [64] to qualitatively validate the PSII light harvesting and photochemistry implementation of the model. Changes in our simulated steady-state O_2 evolution rates are in quantitative agreement with the experimental data, during low light and exceed measured rates under light saturation by ca. 20 % (Fig. S4). Unfortunately, the exact culture conditions (e.g. density) and strain used in the reference work [64] are not known. Hence the pigment composition may differ. We also calculated the fraction of open PSII for increasing light intensities to assess the model quality (Fig. S5). We observed that our response curve is less sensitive to increasing light, as our PSII are open for higher light intensities than reported 300 µmol(photons) $m^{-2}\,s^{-1}$ [65].

Flux through alternative electron pathways

We simulated the steady-state flux of electrons through the PETC for four transport pathways under 670 nm monochromatic illumination (Fig. 1b). We parameterized the flux through the LET to yield approximately 15 electrons $PSI^{-1}\,s^{-1}$ and 60 % of the total PSI electron flux in the wild type (WT) [46]. Our simulated saturation of CET around 300 µmol(photons) $m^{-2}\,s^{-1}$ compares well to proton flux measurements by Miller *et al.* [65]. Under ambient CO_2 (400 ppm), our model simulates an overall limitation of electron flux and an increase in alternative flows. We found similar electron partitioning between WT and in the *Flv1/3* mutant at lower light intensities agreeing with the findings of Theune *et al.* [46]. However, our simulations show significant AEF in the WT over 200 µmol(photons) $m^{-2}\,s^{-1}$, which might have been suppressed by high CO_2 and pH in the experiments by Theune *et al.* (personal correspondence, see also [66]).

Under intermediate light intensity, the *Flv1/3* mutant also showed a higher CET while maintaining LET similar to the WT, pointing towards a balancing act of NDH-1. Inversely, our simulated NDH-1 mutant maintained high AEF but, in contrast to Theune *et al.*, significant flux through the LET. In addition to simulating electron flow, our model can probe the intracellular redox state, pH, and additional fluxes through key biochemical reactions (Fig. S8). For example, it can be seen that a reduced PQ pool under high light leads to reduced CET mediated by NDH-1 and, in turn, a decreased CBB flux due to insufficient provision of ATP. Furthermore, we find that mutations affecting the electron flow lead to an increased Non-Photochemical Quenching (NPQ) at higher light intensities and the decrease in photosynthetic yield (Fig. S7).

Photosynthesis dynamics captured via fluorescence measurements

Using experimental measurements (pigment concentrations, photosystem ratios, and expected PBS-attachment - method currently under review)[56], we manually fitted model parameters to represent a *Synechocystis* strain grown under 435 nm monochromatic light. With this model, we simulate fluorescence in a PAM-SP light protocol [22], which investigates photosynthesis behavior using the dark-adapted minimal (F_0) and maximal fluorescence (F_m), the maximal fluorescence in the light (F'_m) and the constantly measured steady-state fluorescence (F). By monitoring cell responses to changing light conditions, we captured light responses via state transitions and non-photochemical quenching and relaxation (for a review of the mechanisms, see [3] and for related models in plants [15]). We simulated the same light protocol of blue and red light, as used *in vivo* [56], and fit parameters controlling the fluorescence composition, state transitions, and NPQ to cells grown under 435 nm light (Fig. 2a). Our simulation qualitatively reproduces the transition between states 1 and 2 and the activation and relaxation of NPQ by the Orange Carotenoid Protein (OCP). Because our model underestimates PSII

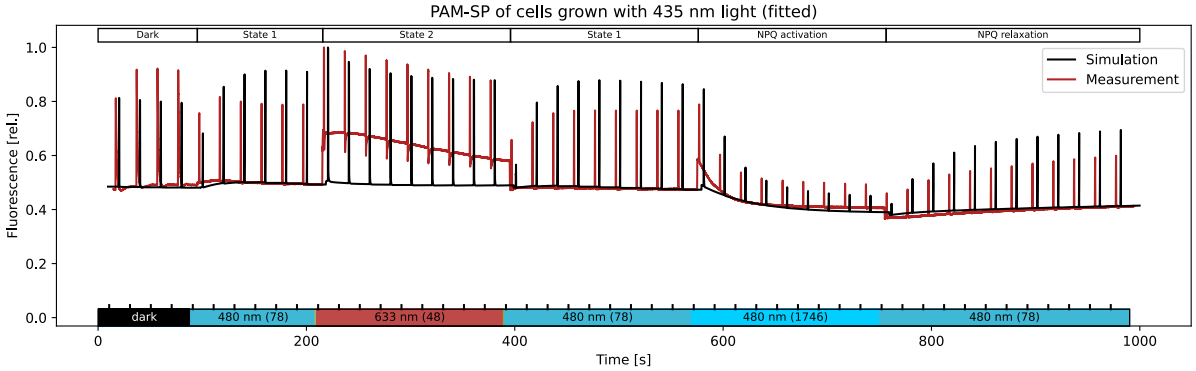

(a) Fit of simulated (black) to measured (red) PAM fluorescence dynamics during a saturation pulse light protocol. The simulation was manually fit using seven model parameters, and the parameters are used for all other model simulations. The experimental traces were measured in *Synechocystis* sp. PCC 6803 grown under 435 nm light (n=2) [56]. Simulations use the measured pigment contents and ambient CO_2 (400 ppm). The shown light protocol includes several different light wavelengths and intensities to trigger a response from respective photosynthetic electron transport chain components. By monitoring cell responses to these light conditions, we captured light responses via state transitions and non-photochemical quenching and relaxation (as described in the upper bar). We calculated light attenuation in the culture using Equation S67 with the measured pigment concentrations and sample chlorophyll content in Table S4.

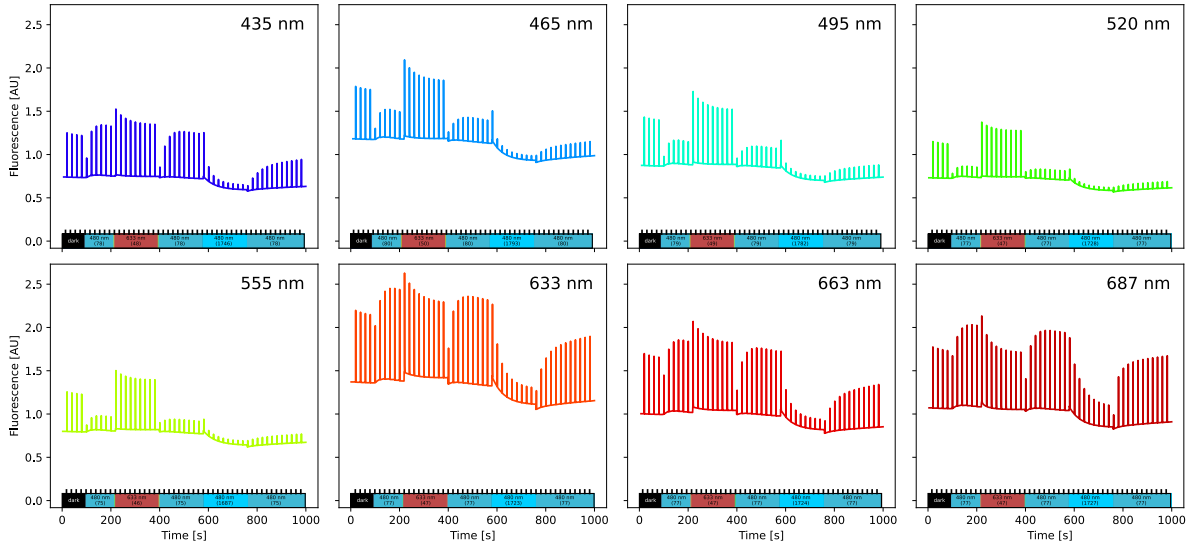

(b) Model prediction on emitted fluorescence signal. Light protocol in a) is repeated with pigment contents measured in cells grown under different monochromatic lights [56]. We calculated light attenuation with the chlorophyll content measured in each culture.

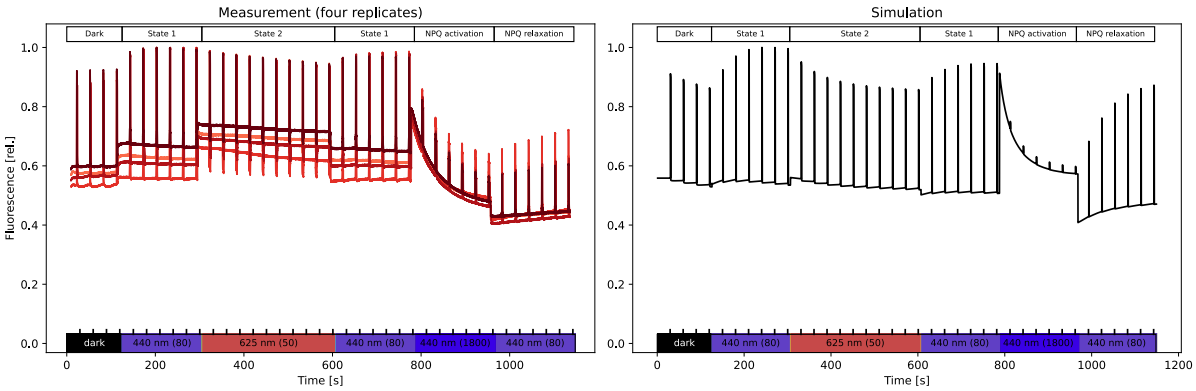

(c) Model validation comparing PAM-SP fluorescence traces *in vivo* and *in silico*. Four experimental replicates are shown. Simulations assume 1 % CO_2 supplementation and use the default parameters (see a)) and pigment set. The model reproduces the fluorescence dynamics during most of the experiment except for overestimating steady-state fluorescence during the strong blue light phase. The lower bar depicts the light wavelength and intensity (in parentheses, in µmol(photons) m^{-2} s^{-1}) (lights used: 440 nm at 80 µmol(photons) m^{-2} s^{-1} and 1800 µmol(photons) m^{-2} s^{-1} and 625 nm at 50 µmol(photons) m^{-2} s^{-1}, saturating pulse: 600 ms cool white LED at 15 000 µmol(photons) m^{-2} s^{-1}). The measurements were performed with a Multi-Color PAM (Walz, Effeltrich, Germany). Cultures of *Synechocystis* sp. PCC 6803 were grown under bubbling with 1 % CO_2 and 25 µmol(photons) m^{-2} s^{-1} of 615 nm light for ca. 24 h. For the measurement, 1.5 mL culture was transferred to a quartz cuvette and dark-acclimated for 15 min prior to each measurement.

Fig. 2: **Saturation pulse method using Pulse Amplitude Modulation (PAM) fluorescence measurement *in vivo* and *in silico*.** The simulated signal has been calculated using (Equation 8). All experimental measurements were performed with a Multi-Color PAM (Walz, Effeltrich, Germany).

closure in response to light, the steady-state fluorescence during light phases is also underestimated. By systematically comparing our simulation results and experimental data, we have revealed that the experimentally used saturation pulses were non-saturating in 480 nm actinic light and induced fluorescence quenching, as confirmed by follow-up experiments (see Fig. S14 in [56] and Fig. S6 in this work). Thus, we found the model's usefulness in investigating fluorescence measurements. Using the same fitted parameters, we can also reproduce the quantitative behavior of cells grown under 633 nm monochromatic light (Fig. S3) and predict the fluorescence under further adapted pigment contents (Fig. 2b). The model shows a strong effect on cellular reactions and fluorescence when adapted to pigment contents of cells grown under other monochromatic lights. We have further validated our model against the newly measured fluorescence trace Fig. 2c. Our simulations predict accurately F'_m, but overestimate fluorescence signal in high 440 nm light (Fig. 2c).

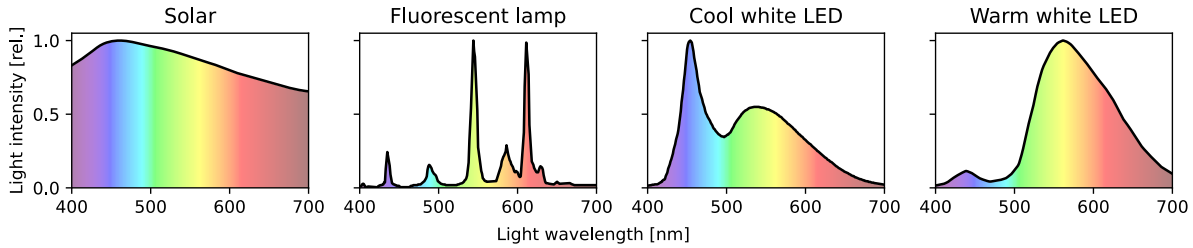

(a) The light spectra of four light sources used in simulations, including common "white" light LED panels.

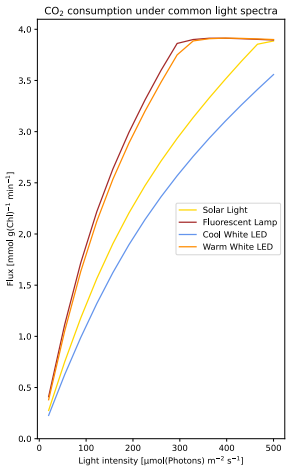

(b) Steady-state flux through the CBB under the lights in (a), simulated over different light intensities.

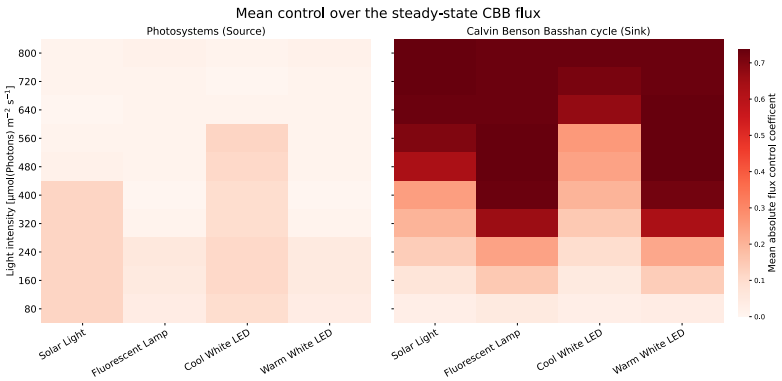

(c) Results of Metabolic Control Analysis (MCA) performed for given light sources with a range of intensities from 80 to 800 µmol(photons) m^{-2} s^{-1} to steady-state. By varying the photosystem concentrations and the maximal rate of the CBB by ± 1 %, we quantified their control on the CBB flux by calculating flux control coefficients. We display the mean of absolutes of control coefficients. Higher values signify stronger pathway control.

Fig. 3: **Systematic analysis of the effect of various light sources on the rate of carbon fixation.**

Common light sources affect the metabolic control differently

Photosynthesis experiments can be conducted with many different light sources that are equivalent in photon output but differ in the spectrum. To further investigate how these spectral differences affect cellular metabolism, we simulated the model with different monochromatic and "white" light sources: solar irradiance, fluorescent lamp, and cool and warm white LED (Fig. 3a). For each light, we simulated the model to steady-state to perform MCA (Fig. 3c). We perturbed single parameters of the PETC components by ± 1 % and quantified the effect on the steady-state fluxes and concentrations. A high control coefficient represents a strong dependency of the pathway flux on changes to that parameter, with control in a metabolic network being distributed across multiple reactions. A single parameter being in full control of the flux through a network would represent the case of a typical bottleneck, but this rarely occurs in biological systems [43, 45]. We show that the electron pathway-specific control differs between the simulated light sources. Our results indicate that, at lower intensities of solar and cool white LED light, the control mainly lies within the photosystems as sources of energy carriers (Fig. 3c). We find less control by the photosystems for light spectra with a higher proportion of red wavelengths, suggesting

such light sources induce less source limitation. Accordingly, the maximal simulated CO_2 consumption is reached at lower light intensities for these spectra (Fig. 3b). All tested spectra show the CBB having the main control of CO_2 fixation only under increased light, marking a shift towards the energy carrier sink limitation.

Repeating the analysis with simulated monochromatic lights, we found similar differences that seem to correspond with the preferential absorption by either chlorophyll or PBS (Fig. S11). The earliest switch to sink limitation was found in 624 nm light, while light that is weakly absorbed by photosynthetic pigments, such as 480 nm, seems to have little control effect. Our analysis also confirmed the intuitive understanding that remaining respiration under low light could have low control on the CBB while alternate electron flow became influential under light saturation (Fig. S10). Using the model, the control of single components, such as photosystems, can also be investigated (Fig. S12).

Model as a platform to test alternative mechanisms of state transition

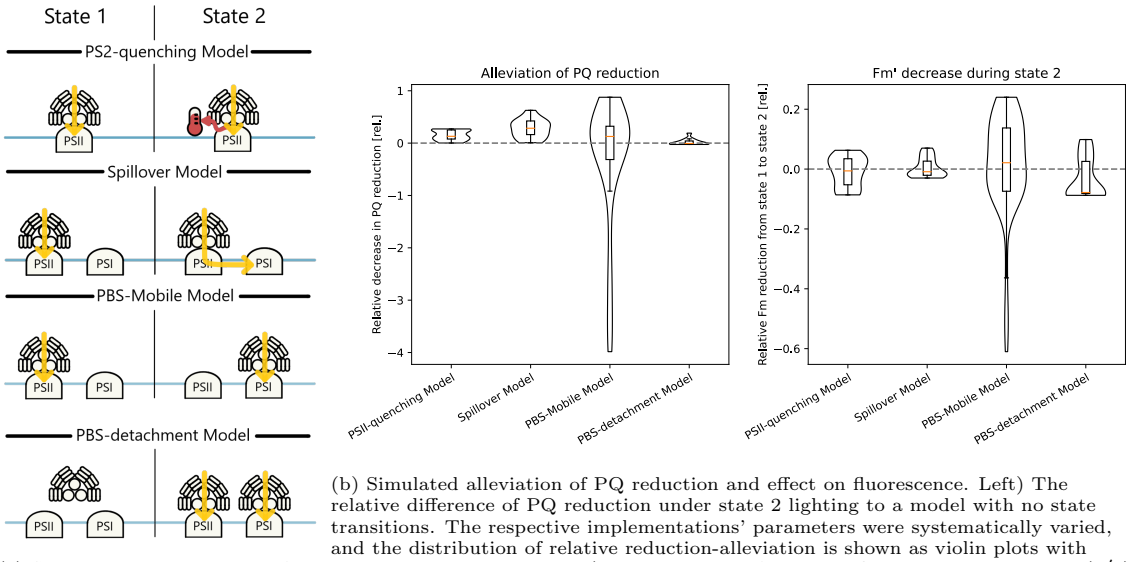

(a) Schematic representation of four state transition models, as reviewed in [42].

(b) Simulated alleviation of PQ reduction and effect on fluorescence. Left) The relative difference of PQ reduction under state 2 lighting to a model with no state transitions. The respective implementations' parameters were systematically varied, and the distribution of relative reduction-alleviation is shown as violin plots with quantiles as boxplots. Right) The reduction of maximal fluorescence in the light (F'_m) from state 1 to state 2 in the model variations. The distribution is also shown as violin plots with inset boxplots.

Fig. 4: **Testing possible mechanisms of state transitions.** Four possible mechanisms of state transitions have been implemented and parameterized randomly to quantify their performance by contributing to oxidising PQ pool. The fluorescence signal has been calculated using (Equation 8).

We defined four functions representing the mechanism of state transitions with the PSII-quenching model [67] as the default. Therein, a higher fraction of PSII excitations is lost as heat in state 2. Three alternative models of state transition were tested: the Spillover Model, where state 2 induces PSII excitation energy transfer to PSI; the PBS-Mobile model, where PBS attach preferentially to PSII or PSI in states 1 and 2, respectively; and the PBS-detachment Model, where PBS detach from the photosystems in state 1 [67, 42]. We model the transition to state 2 under a reduced PQ pool while oxidized PQ promotes state 1. To test the general behavior of these mechanisms without limitation to a single parameter set, we systematically simulated each mechanism with a range of parameter values, typically varying each parameter within two orders of magnitude. We calculated the relative difference of PQ reduction under state 2 lighting to a model with no state transitions, and the reduction of F'_m from state 1 to state 2 (Fig. 4b left). We see that all models can alleviate the PQ reduction that cyanobacteria encounter in state 2. However, across all parameter variations, the PBS-detachment model has vastly lower simulated potential to alleviate the reduction. Variations of the PBS-mobile model simulated a wide range of effects on the redox state, from near total oxidation to increased reduction. During the transition to state 2, the height of F_m is expected to decrease, which all models can simulate within their parameter variations (Fig. 4b right). Again, the simulations of the PBS-mobile model had the widest wide range of simulation results.

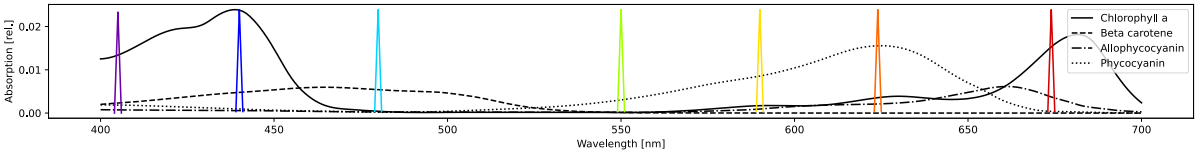

(a) Monochromatic lights used in the analysis (Gaussian LED, $\sigma = 0.001$) shown as colored spikes. Relative absorption spectra of selected pigments are shown in the background.

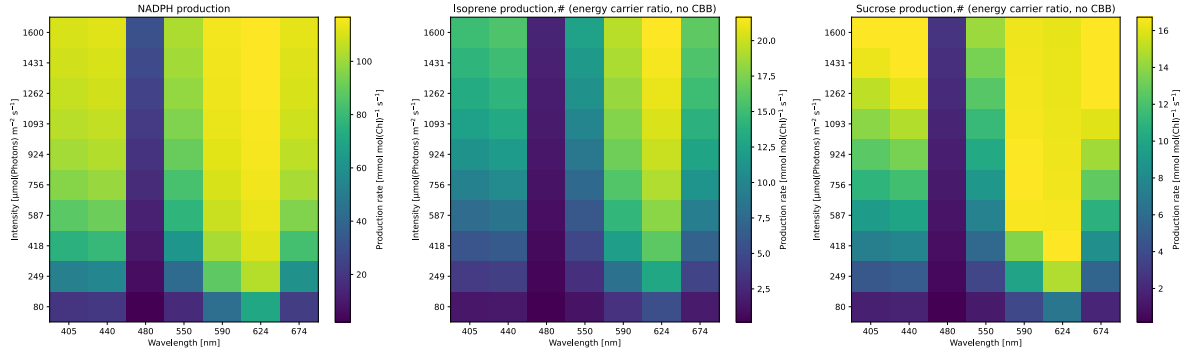

(b) Simulated production capacities of biotechnological compounds under light variation. We created three models, each containing a sink reaction consuming energy carriers in the ratio corresponding to a biotechnological target compound, including the cost of carbon fixation. The models were simulated to steady-state under illumination with varying intensity of the lights in (a). We disabled the CBB reaction and limited ATP and NADPH concentrations to 95 % of their total pools. Thus we estimate the maximal production rate of energy carriers in a desired ratio, assuming optimal carbon assimilation for the process and no product inhibition. The shown sinks represent pure NADPH extraction, production of terpenes (19 ATP, 11 NADPH, 4 Fd_{red}), and sucrose (19 ATP, 12 NADPH).

Fig. 5: **Simulated steady-state production rates of target compounds under monochromatic lights with varying intensities.**

Model as a platform to test optimal light for biotechnological exploration

Cyanobacteria show potential as cell factories for the production of terpenoids from CO_2 or as whole-cell biocatalysts, which require different ratios of NADPH, ATP, and carbon. Several studies revealed that light availability is one of the main limitations of light-driven whole-cell redox biocatalysis [68]. With our model, we systematically analyzed the *Synechocystis* productivity for various light sources.

To identify potentially optimal light conditions and/or quantify the maximal production capacities for these exemplary processes, sink reactions were added to the model, and production was simulated with different light conditions (Fig. 5). These sinks drained the required amounts of ATP,NADPH, and Fd necessary for fixing the required amount of CO_2 and producing one unit of the target compound. Additionally, it was necessary to add reactions that avoid overaccumulation of ATP and NADPH in case the sink was not sufficiently consuming both. The model simulates that NADPH production was highest under red (624 nm) illumination saturating around 800 µmol(photons) m^{-2} s^{-1}. We also compared the simulated productions of isoprene and sucrose, which require different optimal rations of ATP and NADPH, 1.46 and 1.58, respectively. Isoprene production showed a stronger dependency on red-wavelength light, exceeding the production in blue light twofold, and did not saturate within the simulated light intensity range. Presumably, the involvement of Fd as a substrate further favors the usage of light preferentially exciting PSII. In line with the recent work by Rodrigues *et al.* (2023) [29], our simulated isoprene also follows the measured cellular growth rate as predicted by their stoichiometric model analysis (Fig. S13). Accordingly, Rodrigues *et al.* discuss that their experimentally realized isoprene production was determined not just by differential excitation of photosystems. On the other hand, simulation of the more ATP-intensive sucrose production was saturated at much lower light intensities and even decreased slightly under high light. These simulations indicate that the optimal light intensity could be lower for synthesis reactions requiring more ATP. It has also been suggested that the ATP:NADPH ratio is increased under blue light due to higher CET activity [69, 70]. However, our model did not show a benefit of more chlorophyll-absorbed light on the reactions involving ATP. Overall we found 624 nm light, to have the highest simulated production across the tested compounds and lights.

While these results were obtained for an unadapted cell, our model allows us to repeat such analyses with any adapted pigment composition (comparison of estimated CO_2 consumptions in S9).

Discussion

In this work, we present the first wavelength-dependent mathematical ODE-based photosynthesis model for cyanobacteria. The model contains all major processes involved in the *Synechocystis* photosynthetic electron flow, from light capture to CO_2 fixation [17] and a description of the respiratory chain embedded within the same membrane. Furthermore, cyanobacteria-specific mechanisms were implemented in the model, including state transitions and OCP-mediated NPQ [3, 39, 71, 42]. In contrast to other existing dynamic models of photosynthesis, our model takes pigment composition of the strain as an input and can simulate illumination within the full visible spectrum (400-700 nm). Hence, results obtained with our model provide insights into the intricate dynamics of the photosynthetic process under various light conditions.

The model was validated against published measurements of gas exchange rates (Fig. S4) and compared to *in vivo* electron pathway fluxes and cellular fluorescence. The quantitative agreement with oxygen production rates supports our pigment-specific implementation of light absorption, which allows for a better assessment of the possible effect of photosystem imbalance [38, 59]. After parameterizing the model to reproduce the electron fluxes in the wild type, we used it to gain in-depth information on the system's behavior using *in-silico* mutants. Simulations of a Flv knockout mutant showed increased CET by NDH-1 under intermediate light (Fig. 1b). It was reported previously that the proteins provide redundancy for alleviating redox stress [55, 72]. Furthermore, in the Flv mutant, flux from PSII is decreased due to lack of electron outflow to Flv (see Fig. S7). The decreased PSII flux is accompanied by raised NPQ under high light intensities.

Our calculated PAM fluorescence signal is composed of signals originating from both photosystems and PBS, with a similar contribution as in the previously published model [26]. We employed this fluorescence estimate to fit a PAM-SP experiment inducing state transitions and OCP quenching (Fig. 2a). We reached a qualitative agreement in the fluorescence dynamics, especially during the induction of OCP. Therefore, despite existence of more detailed models of OCP dynamics [31], we decided to keep our two-state implementation. The description of state transitions is challenging, as there currently is no literature consensus on the mechanism of state transitions [3, 42]. Therefore, we used our model to compare the implementations of four proposed mechanisms based on the cellular redox state and fluorescence. Simulations of all mechanisms could reproduce the expected cellular effects in some form. We saw, however, that the movement of PBS had the highest dynamic range of reducing or oxidizing the PQ pool, while PBS detachment in state 2 had a very modest effect. Therefore, the targeted movement of PBS could provide the cell with high control over its electron transport. The significance of PBS movement has been debated, however [73, 74, 75, 76], as has the spillover of energy between the photosystems [73, 74, 75]. It is noteworthy that considering solely the effect on PQ redox state, the implemented PSII-quenching model favored by Calzadilla *et al.* [42] does not have a significantly greater effect on the oxidation of PQ in our simulations. This limited PQ oxidation is in line with a model of plant photoinhibition where PSII quenching decreased PSII closure by ca. 10 % [77]. Overall, the mechanism of state transitions and its impact on photosynthetic balance remains to be evaluated.

Therefore, we used MCA to systematically study the effect of light (intensity and color) and determined the systems control on carbon fixation considering varying illumination: solar illumination, a fluorescent lamp, and cold and warm white LEDs (Fig. 3) of different intensities. The photosystems mainly controlled carbon fixation in simulations of low light intensity, which is in line with the limitation of light uptake and ATP and NADPH production as found in analyses of plant models [48]. Spectra with a high content of blue wavelength photons, which have been linked with an imbalanced excitation of PSI and PSII [37], showed a further increase in photosystems control. Indeed, blue light was found to increase PSII expression [78, 69], a cellular adaption possibly using this control. At higher light intensities, the maximum rate of carbon fixation became the main controlling factor. Thus, the strategy promising better productivity would involve increasing carbon fixation by e.g. additionally increasing the CO_2 concentration around RuBisCO [79], engineering RuBisCO itself [80] or introducing additional electron acceptors and carbon sinks such as sucrose, lactate, terpenoids or 2,3-butanediol [81, 82, 83, 84, 85].

With the implementation of the spectral resolution, our model could also simulate cellular behavior in high cell densities (e.g. bioreactors), where the light conditions might differ throughout the culture [86]. We show that lighting in the orange-red spectrum requires the lowest intensity to saturate the photosystems, with a warm-white LED showing the same efficiency as a fluorescent light bulb, an important consideration when calculating process costs (Fig. 3b).

To showcase the biotechnological usability of this work, we analyzed the *Synechocystis* productivity for various light sources (Fig. 5). Many experimental studies have investigated optimal light colors for

the production of biomass or a target compound, with most studies agreeing that white or red light is optimal for cell growth but varying results for target compounds [87, 88, 29]. Especially the synthesis of light harvesting or protection pigments is regulated and strongly dependent on the light color [89, 90, 91, 92]. These works point out that biotechnological production can be strongly improved using "correct" lighting. However, finding such optimal experimental conditions may be hindered by, for example, the active regulation of pigment synthesis - processes that could be overcome by cellular engineering. Using our model of a cell without long-term adaption, we may identify optimal conditions to aim for in cell engineering and experimentation. By simulating a target compound consuming the amount of ATP, NADPH and reduced Ferredoxin (Fd) necessary to synthesize the target compound from carbon fixation, we tried to estimate the maximum production potential without limitation by the CBB. We found that the simulated production of all three compounds was highest under red light illumination (624 nm). Sucrose production was saturated at intermediate light and even showed slight inhibition under high light, while the simulated isoprene production, requiring reduced Fd and a lower amount of ATP, showed the highest requirement for light (no saturation at 1600 µmol(photons) m^{-2} s^{-1}). Thus, the composition of energy equivalents seems to determine the optimal lighting conditions. NADPH production in particular seemed to follow a light saturation curve with maximum around 1600 µmol(photons) m^{-2} s^{-1} For the purpose of whole-cell biocatalysis, NADPH is often the only required cofactor for the reaction, while the generation of ATP and biomass are secondary. Studies have attempted to optimise NADPH regeneration through inhibition of the CBB, deletion of flavodiiron proteins, or introducing additional heterologous sinks for ATP, while at the same time trying to avoid oxidative stress [93, 94, 95]. Our simulations suggest that a switch in light color towards monochromatic red light may be a viable strategy to improve catalysis by matching the NADPH-focused demand of the sink reaction with an equally biased source reaction.

These results again support the need to test and optimize light conditions for each application on its own, as the stoichiometry of the desired process changes light requirements. Recently, two-phase processes have been used to increase titers in cyanobacterial biotechnology, arresting growth to direct all carbon towards a product [96]. Our model suggests that as a part of this process, changes in light color could be used to intentionally create imbalances in metabolism and direct flux to the desired product according to the energetic needs of the particular pathway.

To address the limitations of current model, it is imperative to critically evaluate its underlying assumptions and identify key areas for improvement. For instance, withe the current version of the model we cannot predict the long-term cellular adaption governed by many photoreceptors [97, 98]. For each simulation, we assume fixed pigment composition and light absorption capacity, thus, analysing a given cell state. Relevant cellular adaptions can, however, be used as new inputs according to experimental data. Also, rhodopsin photoreceptors can perform light-driven ion transport and, if found photosynthetically relevant, would be a useful addition to the model [99, 100]. Next, although our model considers the CBB as the main sink for energy equivalents, reactions downstream of the CBB, such as glycogen production [101]), could pose additional significant sinks depending on the cell's metabolic state, necessitating further refinement of our model to accurately capture these dynamics. Additionally, further improvements of the currently significantly simplified CCM (Fig. S2) and photorespiratory salvage functions could be beneficial, also due to the engineering efforts in building pyrenoid-based CO_2-concentrating mechanisms *in-planta* [102]. Photodamage may be a necessary addition to the model when considering high-light conditions, specifically PSII photoinhibition and the Mehler reaction [103] (see i.e. [30]). Finally, our model follows the dynamic change in the lumenal and cytoplasmic pH but is lacking the full description of *pmf*. An envisaged step of further development will be the integration of the membrane potential $\Delta\Psi$ into the model and simulation of ion movement, as presented in several mathematical models for plants [18, 104]. It would be moreover interesting to include the spatial component into the model, accounting for the dynamics of thylakoid membranes, as revealed by [105]. Thanks to our computational implementation of the model using the package `modelbase` [51], the model is highly modular, and the addition of new pathways or the integration of other published models (e.g. a recent CBB model [106]) should not constitute a technical challenge.

In conclusion, the development of our first-generation computational model for simulating photosynthetic dynamics represents a significant advancement in our comprehension of cyanobacteria-specific photosynthetic electron flow. While acknowledging its imperfections, our model has proven to be a versatile tool with a wide range of applications, spanning from fundamental research endeavors aimed at unravelling the complexities of photosynthesis to practical efforts focused on biotechnological optimization. Through a comprehensive presentation of our results, we have demonstrated the model's capacity to elucidate core principles underlying photosynthetic processes, test existing hypotheses, and offer valuable insights on the photosynthetic control under various light spectra. With further

development and integration of experimental data, we hope to provide a reference kinetic model of cyanobacteria photosynthesis.

Acknowledgements

We would like to thank Ilka Axmann and Marion Eisenhut for the initial conversations on the physiology of cyanobacteria that motivated the construction of this detailed model, and David Fuente for the discussion on the cyanobacterial absorption and pigment compositions.

Funding statement

This work was funded by the Deutsche Forschungsgemeinschaft under Germany´s Excellence Strategy – EXC-2048/1 – project ID 390686111 (TP, OE, AM); Deutsche Forschungsgemeinschaft Research Grant - project ID 420069095 (EK, AN, AM); Ministry of Education, Youth and Sports of CR within the CzeCOS program (grant number LM2018123), under the OP RDE (grant number CZ.02.1.01/0.0/0.0/16 026/0008413 'Strategic Partnership for Environmental Technologies and Energy Production') (TZ, JC); as well as by the National Research, Development and Innovation Office of Hungary, NKFIH (awards K 140351 and RRF-2.3.1-21-2022-00014 (GB).

Authors contribution

TP, EK developed the computational model; TP, EK and AN performed simulations and visualizations; TZ performed validation experiments and performed data curation; OE, AM, JC, GB acquired funding; TP, EK, AN, and AM wrote the original draft; TP and AM reviewed and edited the corrected manuscript; AM conceptualized, initiated and supervised the project; all authors were involved in discussions on methodology and investigation and made a substantial, direct, and intellectual contribution to the work and approved it for publication.

References

[1] Malihe Mehdizadeh Allaf and Hassan Peerhossaini. Cyanobacteria: Model Microorganisms and Beyond, 4 2022.

[2] Sophie De Vries and Jan De Vries. Evolutionary genomic insights into cyanobacterial symbioses in plants, 8 2022.

[3] Alexandrina Stirbet, Dušan Lazár, George C. Papageorgiou, and Govindjee. Chapter 5 - Chlorophyll a Fluorescence in Cyanobacteria: Relation to Photosynthesis. In A. K. Mishra, D. N. Tiwari, and A. N. Rai, editors, *Cyanobacteria*, pages 79–130. Academic Press, January 2019.

[4] Jay Kumar, Divya Singh, Madhu B. Tyagi, and Ashok Kumar. Cyanobacteria: Applications in Biotechnology. In *Cyanobacteria*, chapter 16, pages 327–346. Elsevier, 12 2019.

[5] K Benedikt Möllers, David Cannella, Henning Jørgensen, and Niels-Ulrik Frigaard. Cyanobacterial biomass as carbohydrate and nutrient feedstock for bioethanol production by yeast fermentation. *Biotechnology for Biofuels*, 7(1):64, 12 2014.

[6] Stephanie G. Hays and Daniel C. Ducat. Engineering cyanobacteria as photosynthetic feedstock factories. *Photosynthesis Research*, 123(3):285–295, 3 2015.

[7] Mrinal Kumar Sarma, Sharbani Kaushik, and Pranab Goswami. Cyanobacteria: A metabolic power house for harvesting solar energy to produce bio-electricity and biofuels. *Biomass and Bioenergy*, 90:187–201, 7 2016.

[8] Ewa Żymańczyk-Duda, Sunday Ocholi Samson, Małgorzata Brzezińska-Rodak, and Magdalena Klimek-Ochab. Versatile Applications of Cyanobacteria in Biotechnology. *Microorganisms*, 10(12), 12 2022.

[9] Oliver Klaus, Fabienne Hilgers, Andreas Nakielski, Dennis Hasenklever, Karl Erich Jaeger, Ilka M. Axmann, and Thomas Drepper. Engineering phototrophic bacteria for the production of terpenoids. *Current Opinion in Biotechnology*, 77:102764, 10 2022.

[10] Jens Appel, Vanessa Hueren, Marko Boehm, and Kirstin Gutekunst. Cyanobacterial in vivo solar hydrogen production using a photosystem I–hydrogenase (PsaD-HoxYH) fusion complex. *Nature Energy*, 5(6):458–467, 6 2020.

[11] David J Lea-Smith, Paolo Bombelli, Ravendran Vasudevan, and Christopher J Howe. Photosynthetic, respiratory and extracellular electron transport pathways in cyanobacteria. *Biochimica et Biophysica Acta (BBA) - Bioenergetics*, 1857(3):247–255, 3 2016.

[12] Christine M. Lewis, Justin D. Flory, Thomas A. Moore, Ana L. Moore, Bruce E. Rittmann, Wim F.J. Vermaas, César I. Torres, and Petra Fromme. Electrochemically Driven Photosynthetic Electron Transport in Cyanobacteria Lacking Photosystem II. *Journal of the American Chemical Society*, 144(7):2933–2942, 2 2022.

[13] David M. Kramer and John R. Evans. The importance of energy balance in improving photosynthetic productivity. *Plant Physiology*, 155(1):70–78, 2011.

[14] Andreas Karoly Gombert and Jens Nielsen. Mathematical modelling of metabolism. *Current Opinion in Biotechnology*, 11(2):180–186, 4 2000.

[15] Alexandrina Stirbet, Dušan Lazár, Ya Guo, and Govindjee Govindjee. Photosynthesis: Basics, history and modelling. *Annals of Botany*, 126(4):511–537, 2020.

[16] Thierry Fourcaud, Xiaopeng Zhang, Alexia Stokes, Hans Lambers, and Christian Körner. Plant growth modelling and applications: The increasing importance of plant architecture in growth models, 5 2008.

[17] David J. Lea-Smith and Guy T. Hanke. Electron Transport in Cyanobacteria and Its Potential in Bioproduction. In *Cyanobacteria Biotechnology*, pages 33–63. Wiley, 5 2021.

[18] Meng Li, Vaclav Svoboda, Geoffry Davis, David Kramer, Hans Henning Kunz, and Helmut Kirchhoff. Impact of ion fluxes across thylakoid membranes on photosynthetic electron transport and photoprotection. *Nature Plants*, 7(7):979–988, 7 2021.

[19] Robert L. Burnap, Martin Hagemann, and Aaron Kaplan. Regulation of CO2concentrating mechanism in cyanobacteria, 1 2015.

[20] Jinlan Gao, Hao Wang, Qipeng Yuan, and Yue Feng. Structure and Function of the Photosystem Supercomplexes. *Frontiers in Plant Science*, 9:357, 3 2018.

[21] E. M. Sukhova, V. A. Vodeneev, and V. S. Sukhov. Mathematical Modeling of Photosynthesis and Analysis of Plant Productivity. *Biochemistry (Moscow), Supplement Series A: Membrane and Cell Biology*, 15(1):52–72, January 2021.

[22] Ulrich Schreiber. Pulse-Amplitude-Modulation (PAM) Fluorometry and Saturation Pulse Method: An Overview. In *Chlorophyll a Fluorescence*, number January 2004, pages 279–319. Springer Netherlands, Dordrecht, 2004.

[23] Douglas Campbell, Vaughan Hurry, Adrian K. Clarke, Petter Gustafsson, and Gunnar Öquist. Chlorophyll Fluorescence Analysis of Cyanobacterial Photosynthesis and Acclimation. *Microbiology and Molecular Biology Reviews*, 62(3):667–683, 9 1998.

[24] D. Lazar, A. Stirbet, L. O. Björn, and G. Govindjee. Light quality, oxygenic photosynthesis and more. *Photosynthetica*, 60(SPECIAL ISSUE 2022):25–58, March 2022. Publisher: Photosynthetica.

[25] R. Milou Schuurmans, Pascal van Alphen, J. Merijn Schuurmans, Hans C. P. Matthijs, and Klaas J. Hellingwerf. Comparison of the Photosynthetic Yield of Cyanobacteria and Green Algae: Different Methods Give Different Answers. *PLOS ONE*, 10(9):e0139061, 9 2015.

[26] Alonso M. Acuña, Joris J. Snellenburg, Michal Gwizdala, Diana Kirilovsky, Rienk van Grondelle, and Ivo H. M. van Stokkum. Resolving the contribution of the uncoupled phycobilisomes to cyanobacterial pulse-amplitude modulated (PAM) fluorometry signals. *Photosynthesis Research*, 127(1):91–102, 1 2016.

[27] Stefanie Westermark and Ralf Steuer. Toward Multiscale Models of Cyanobacterial Growth: A Modular Approach. *Frontiers in Bioengineering and Biotechnology*, 4:95, 12 2016.

[28] Henning Knoop, Yvonne Zilliges, Wolfgang Lockau, and Ralf Steuer. The Metabolic Network of Synechocystis sp. PCC 6803: Systemic Properties of Autotrophic Growth. *Plant Physiology*, 154(1):410–422, 9 2010.

[29] João S. Rodrigues, László Kovács, Martin Lukeš, Rune Höper, Ralf Steuer, Jan Červený, Pia Lindberg, and Tomáš Zavřel. Characterizing isoprene production in cyanobacteria – Insights into the effects of light, temperature, and isoprene on Synechocystis sp. PCC 6803. *Bioresource Technology*, 380:129068, 7 2023.

[30] R. Höper, D. Komkova, T. Zavřel, and R. Steuer. A quantitative description of light-limited cyanobacterial growth using flux balance analysis, January 2024.

[31] Maxim Y Gorbunov, Fedor I Kuzminov, Victor V Fadeev, John Dongun Kim, and Paul G Falkowski. A kinetic model of non-photochemical quenching in cyanobacteria. *Biochimica et Biophysica Acta - Bioenergetics*, 1807(12):1591–1599, 2011.

[32] A V Vershubskii, V I Mishanin, and A N Tikhonov. Modeling of the photosynthetic electron transport regulation in cyanobacteria. *Biochemistry (Moscow) Supplement Series A: Membrane and Cell Biology*, 31(2):110–128, 7 2014.

[33] Tomáš Zavřel, Marjan Faizi, Cristina Loureiro, Gereon Poschmann, Kai Stühler, Maria Sinetova, Anna Zorina, Ralf Steuer, and Jan Červený. Quantitative insights into the cyanobacterial cell economy. *eLife*, 8, feb 2019.

[34] Björn Andersson, Chen Shen, Michael Cantrell, David S. Dandy, and Graham Peers. The fluctuating cell-specific light environment and its effects on cyanobacterial physiology. *Plant Physiology*, 181(2):547–564, 2019.

[35] Marcel Dann, Edgardo M. Ortiz, Moritz Thomas, Arthur Guljamow, Martin Lehmann, Hanno Schaefer, and Dario Leister. Enhancing photosynthesis at high light levels by adaptive laboratory evolution. *Nature Plants*, 7(5):681–695, 5 2021.

[36] Gábor Bernát, Tomáš Zavřel, Eva Kotabová, László Kovács, Gábor Steinbach, Lajos Vörös, Ondřej Prášil, Boglárka Somogyi, and Viktor R Tóth. Photomorphogenesis in the Picocyanobacterium Cyanobium gracile Includes Increased Phycobilisome Abundance Under Blue Light, Phycobilisome Decoupling Under Near Far-Red Light, and Wavelength-Specific Photoprotective Strategies. *Frontiers in Plant Science*, 12:352, 3 2021.

[37] Veerle M Luimstra, J Merijn Schuurmans, Antonie M Verschoor, Klaas J Hellingwerf, Jef Huisman, and Hans C P Matthijs. Blue light reduces photosynthetic efficiency of cyanobacteria through an imbalance between photosystems I and II. *Photosynthesis Research*, 138(2):177–189, 11 2018.

[38] Veerle M. Luimstra, J. Merijn Schuurmans, Carolina F. M. de Carvalho, Hans C. P. Matthijs, Klaas J. Hellingwerf, and Jef Huisman. Exploring the low photosynthetic efficiency of cyanobacteria in blue light using a mutant lacking phycobilisomes. *Photosynthesis Research*, 141(3):291–301, 9 2019.

[39] Diana Kirilovsky and Cheryl A. Kerfeld. The Orange Carotenoid Protein: a blue-green light photoactive protein. *Photochemical & Photobiological Sciences*, 12(7):1135–1143, 7 2013.

[40] Cheryl A. Kerfeld, Matthew R. Melnicki, Markus Sutter, and Maria Agustina Dominguez-Martin. Structure, function and evolution of the cyanobacterial orange carotenoid protein and its homologs. *New Phytologist*, 215(3):937–951, 8 2017.

[41] Diana Kirilovsky, Radek Kaňa, and Ondřej Prášil. Mechanisms Modulating Energy Arriving at Reaction Centers in Cyanobacteria. In Barbara Demmig-Adams, Gyozo Garab, William Adams III, and Govindjee, editors, *Non-Photochemical Quenching and Energy Dissipation in Plants, Algae and Cyanobacteria*, pages 471–501. Springer Netherlands, Dordrecht, 2014.

[42] Pablo I Calzadilla and Diana Kirilovsky. Revisiting cyanobacterial state transitions. *Photochemical & Photobiological Sciences*, 19(5):585–603, 5 2020.

[43] R. Heinrich, S.M. Rapoport, and T.A. Rapoport. Metabolic regulation and mathematical models. *Progress in Biophysics and Molecular Biology*, 32(C):1–82, 1978.

[44] Jan-Hendrik S Hofmeyr. Metabolic control analysis in a nutshell. *Proceedings of the 2nd International Conference on Systems Biology*, (ii):291–300, 2001.

[45] Rafael Moreno-Sánchez, Emma Saavedra, Sara Rodríguez-Enríquez, and Viridiana Olín-Sandoval. Metabolic Control Analysis: A tool for designing strategies to manipulate metabolic pathways. *Journal of Biomedicine and Biotechnology*, 2008(1), 2008.

[46] Marius L. Theune, Sarah Hildebrandt, Anja Steffen-Heins, Wolfgang Bilger, Kirstin Gutekunst, and Jens Appel. In-vivo quantification of electron flow through photosystem I – Cyclic electron transport makes up about 35% in a cyanobacterium. *Biochimica et Biophysica Acta - Bioenergetics*, 1862(3):148353, 2021.

[47] Oliver Ebenhöh, Geoffrey Fucile, Giovanni Finazzi, Jean David Rochaix, and Michel Goldschmidt-Clermont. Short-term acclimation of the photosynthetic electron transfer chain to changing light: A mathematical model. *Philosophical Transactions of the Royal Society B: Biological Sciences*, 369(1640):20130223, apr 2014.

[48] Anna Matuszyńska, Nima P. Saadat, and Oliver Ebenhöh. Balancing energy supply during photosynthesis – a theoretical perspective. *Physiologia Plantarum*, 166(1):392–402, may 2019.

[49] Murray R. Badger and G. Dean Price. CO2 concentrating mechanisms in cyanobacteria: molecular components, their diversity and evolution. *Journal of Experimental Botany*, 54(383):609–622, February 2003.

[50] Guido Van Rossum and Fred L Drake. *Python 3 Reference Manual*. CreateSpace, Scotts Valley, CA, 2009.

[51] Marvin van Aalst, Oliver Ebenhöh, and Anna Matuszyńska. Constructing and analysing dynamic models with modelbase v1.2.3: a software update. *BMC Bioinformatics*, 22(1):203, 12 2021.

[52] Shimshon Belkin, Rolf J. Mehlhorn, and Lester Packer. Proton Gradients in Intact Cyanobacteria. *Plant Physiology*, 84(1):25–30, may 1987.

[53] Jason W. Cooley and Wim F. J. Vermaas. Succinate Dehydrogenase and Other Respiratory Pathways in Thylakoid Membranes of Synechocystis sp. Strain PCC 6803: Capacity Comparisons and Physiological Function. *Journal of Bacteriology*, 183(14):4251–4258, jul 2001.

[54] Sergey Khorobrykh, Tatsuhiro Tsurumaki, Kan Tanaka, Taina Tyystjärvi, and Esa Tyystjärvi. Measurement of the redox state of the plastoquinone pool in cyanobacteria. *FEBS Letters*, 594(2):367–375, jan 2020.

[55] Lauri Nikkanen, Anita Santana Sánchez, Maria Ermakova, Matthias Rögner, Laurent Cournac, and Yagut Allahverdiyeva. Functional redundancy between flavodiiron proteins and NDH-1 in Synechocystis sp. PCC 6803. *The Plant Journal*, 103(4):1460–1476, aug 2020.

[56] Tomáš Zavřel, Anna Segečová, László Kovács, Martin Lukeš, Zoltán Novák, Anne-Christin Pohland, Milán Szabó, Boglárka Somogyi, Ondřej Prášil, Jan Červený, and Gábor Bernát. A comprehensive study of light quality acclimation in Synechocystis sp. PCC 6803, February 2024. Pages: 2023.06.08.544187 Section: New Results.

[57] Wolfram Liebermeister, Jannis Uhlendorf, and Edda Klipp. Modular rate laws for enzymatic reactions: thermodynamics, elasticities and implementation. *Bioinformatics*, 26(12):1528–1534, 6 2010.

[58] Elad Noor, Avi Flamholz, Wolfram Liebermeister, Arren Bar-Even, and Ron Milo. A note on the kinetics of enzyme action: A decomposition that highlights thermodynamic effects. *FEBS Letters*, 587(17):2772–2777, 9 2013.

[59] David Fuente, Dusan Lazar, Jose Vicente Oliver-Villanueva, and Javier F. Urchueguía. Reconstruction of the absorption spectrum of Synechocystis sp. PCC 6803 optical mutants from the in vivo signature of individual pigments. *Photosynthesis Research*, 147(1):75–90, jan 2021.

[60] Jeremy Harbinson and Eva Rosenqvist. An Introduction to Chlorophyll Fluorescence. In *Practical Applications of Chlorophyll Fluorescence in Plant Biology*, pages 1–29. Springer US, Boston, MA, 2003.

[61] Dušan Lazár. A word or two about chlorophyll fluorescence and its relation to photosynthesis research; a text for Ph.D. students, 5 2016.

[62] Christina Evi Pfaffinger, Dennis Schöne, Sascha Trunz, Hannes Löwe, and Dirk Weuster-Botz. Model-based optimization of microalgae areal productivity in flat-plate gas-lift photobioreactors. *Algal Research*, 20:153–163, December 2016.

[63] H. Kacser and J. A. Burns. The control of flux. *Symp Soc Exp Biol*, 27:65–104, 1973.

[64] R. Milou Schuurmans, J. Merijn Schuurmans, Martijn Bekker, Jacco C. Kromkamp, Hans C.P. Matthijs, and Klaas J. Hellingwerf. The redox potential of the plastoquinone pool of the cyanobacterium synechocystis species strain PCC 6803 is under strict homeostatic control. *Plant Physiology*, 165(1):463–475, 2014.

[65] Neil T. Miller, Michael D. Vaughn, and Robert L. Burnap. Electron flow through NDH-1 complexes is the major driver of cyclic electron flow-dependent proton pumping in cyanobacteria. *Biochimica et Biophysica Acta - Bioenergetics*, 1862(3), 3 2021.

[66] Anita Santana-Sanchez, Daniel Solymosi, Henna Mustila, Luca Bersanini, Eva-Mari Aro, and Yagut Allahverdiyeva. Flavodiiron proteins 1–to-4 function in versatile combinations in O2 photoreduction in cyanobacteria. *eLife*, 8, 7 2019.

[67] Reza Ranjbar Choubeh, Emilie Wientjes, Paul C Struik, Diana Kirilovsky, and Herbert van Amerongen. State transitions in the cyanobacterium Synechococcus elongatus 7942 involve reversible quenching of the photosystem II core. *Biochimica et Biophysica Acta (BBA) - Bioenergetics*, 1859(10):1059–1066, 10 2018.

[68] Adrian Tüllinghoff, Harcel Djaya-Mbissam, Jörg Toepel, and Bruno Bühler. Light-driven redox biocatalysis on gram-scale in Synechocystis sp. PCC 6803 via an in vivo cascade. *Plant Biotechnology Journal*, 21(10):2074–2083, 2023. _eprint: https://onlinelibrary.wiley.com/doi/pdf/10.1111/pbi.14113.

[69] Veerle M. Luimstra, J. Merijn Schuurmans, Klaas J. Hellingwerf, Hans C. P. Matthijs, and Jef Huisman. Blue light induces major changes in the gene expression profile of the cyanobacterium Synechocystis sp. PCC 6803. *Physiologia Plantarum*, 170(1):10–26, 2020. _eprint: https://onlinelibrary.wiley.com/doi/pdf/10.1111/ppl.13086.

[70] Chiaki Yamamoto, Masakazu Toyoshima, Sayaka Kitamura, Yoshifumi Ueno, Seiji Akimoto, Yoshihiro Toya, and Hiroshi Shimizu. Estimation of linear and cyclic electron flows in photosynthesis based on 13C-metabolic flux analysis. *Journal of Bioscience and Bioengineering*, 131(3):277–282, March 2021.

[71] Ciaran R. McFarlane, Nita R. Shah, Burak V. Kabasakal, Blanca Echeverria, Charles A. R. Cotton, Doryen Bubeck, and James W. Murray. Structural basis of light-induced redox regulation in the Calvin–Benson cycle in cyanobacteria. *Proceedings of the National Academy of Sciences*, 116(42):20984–20990, 10 2019.

[72] Lauri Nikkanen, Daniel Solymosi, Martina Jokel, and Yagut Allahverdiyeva. Regulatory electron transport pathways of photosynthesis in cyanobacteria and microalgae: Recent advances and biotechnological prospects. *Physiologia Plantarum*, 173(2):514–525, 10 2021.

[73] Pablo I. Calzadilla, Jiao Zhan, Pierre Sétif, Claire Lemaire, Daniel Solymosi, Natalia Battchikova, Qiang Wang, and Diana Kirilovsky. The Cytochrome b6f Complex Is Not Involved in Cyanobacterial State Transitions. *The Plant Cell*, 31(4):911–931, 4 2019.

[74] Igor N. Stadnichuk, Evgeny P. Lukashev, and Irina V. Elanskaya. Fluorescence changes accompanying short-term light adaptations in photosystem I and photosystem II of the cyanobacterium Synechocystis sp. PCC 6803 and phycobiliprotein-impaired mutants: State 1/State 2 transitions and carotenoid-induced quenching of phycobilisomes. *Photosynthesis Research*, 99(3):227–241, March 2009.

[75] Volha Chukhutsina, Luca Bersanini, Eva Mari Aro, and Herbert Van Amerongen. Cyanobacterial Light-Harvesting Phycobilisomes Uncouple From Photosystem I During Dark-To-Light Transitions. *Scientific Reports 2015 5:1*, 5(1):1–10, September 2015.

[76] Sarah Joshua and Conrad W. Mullineaux. Phycobilisome Diffusion Is Required for Light-State Transitions in Cyanobacteria. *Plant Physiology*, 135(4):2112–2119, August 2004.

[77] Tim Nies, Shizue Matsubara, and Oliver Ebenhöh. A mathematical model of photoinhibition: exploring the impact of quenching processes. preprint, Plant Biology, September 2023.

[78] Abhay K. Singh, Maitrayee Bhattacharyya-Pakrasi, Thanura Elvitigala, Bijoy Ghosh, Rajeev Aurora, and Himadri B. Pakrasi. A Systems-Level Analysis of the Effects of Light Quality on the Metabolism of a Cyanobacterium. *Plant Physiology*, 151(3):1596–1608, November 2009.

[79] Nina A Kamennaya, Seeun Ahn, Hanwool Park, Roy Bartal, Kenji A Sasaki, Hoi-Ying Holman, and Christer Jansson. Installing extra bicarbonate transporters in the cyanobacterium Synechocystis sp. PCC6803 enhances biomass production. *Metab. Eng.*, 29:76–85, 5 2015.

[80] Feiyan Liang and Peter Lindblad. Synechocystis PCC 6803 overexpressing RuBisCO grow faster with increased photosynthesis. *Metab Eng Commun*, 4:29–36, 6 2017.

[81] Xiang Gao, Fang Gao, Deng Liu, Hao Zhang, Xiaoqun Nie, and Chen Yang. Engineering the methylerythritol phosphate pathway in cyanobacteria for photosynthetic isoprene production from CO2. *Energy & Environmental Science*, 9(4):1400–1411, 2016.

[82] Masahiro Kanno, Austin L Carroll, and Shota Atsumi. Global metabolic rewiring for improved CO2 fixation and chemical production in cyanobacteria. *Nat. Commun.*, 8:14724, 3 2017.

[83] Amit K. Singh, María Santos-Merino, Jonathan K. Sakkos, Berkley J. Walker, and Daniel C Ducat. Multi-layer Regulation of Rubisco in Response to Altered Carbon Status in Synechococcus elongatus PCC 7942. *bioRxiv*, 10 2021.

[84] Marcel Grund, Torsten Jakob, Jörg Toepel, Andreas Schmid, Christian Wilhelm, and Bruno Bühler. Heterologous Lactate Synthesis in Synechocystis sp. Strain PCC 6803 Causes a Growth Condition-Dependent Carbon Sink Effect. *Appl. Environ. Microbiol.*, 88(8):e0006322, 4 2022.

[85] María Santos-Merino, Alejandro Torrado, Geoffry A. Davis, Annika Röttig, Thomas S. Bibby, David M. Kramer, and Daniel C. Ducat. Improved photosynthetic capacity and photosystem I oxidation via heterologous metabolism engineering in cyanobacteria. *Proceedings of the National Academy of Sciences*, 118(11):e2021523118, March 2021.

[86] Alessandro Cordara, Angela Re, Cristina Pagliano, Pascal Van Alphen, Raffaele Pirone, Guido Saracco, Filipe Branco dos Santos, Klaas Hellingwerf, and Nicolò Vasile. Analysis of the light intensity dependence of the growth of Synechocystis and of the light distribution in a photobioreactor energized by 635 nm light. *PeerJ*, 6:e5256, 7 2018.

[87] Ronaldo Leal Carneiro, Maria Elisângela Venâncio dos Santos, Ana Beatriz Furlanetto Pacheco, and Sandra Maria Feliciano de Oliveira e Azevedo. Effects of light intensity and light quality on growth and circadian rhythm of saxitoxins production in Cylindrospermopsis raciborskii (Cyanobacteria). *Journal of Plankton Research*, 31(5):481–488, May 2009.

[88] Alexandros Polyzois, Diana Kirilovsky, Thi-hanh Dufat, and Sylvie Michel. Effects of Modification of Light Parameters on the Production of Cryptophycin, Cyanotoxin with Potent Anticancer Activity, in Nostoc sp. *Toxins*, 12(12):809, December 2020. Number: 12 Publisher: Multidisciplinary Digital Publishing Institute.

[89] Sanjiv K. Mishra, Anupama Shrivastav, Rahulkumar R. Maurya, Shailesh K. Patidar, Soumya Haldar, and Sandhya Mishra. Effect of light quality on the C-phycoerythrin production in marine cyanobacteria *Pseudanabaena* sp. isolated from Gujarat coast, India. *Protein Expression and Purification*, 81(1):5–10, January 2012.

[90] George N. Hotos and Theodoros I. Antoniadis. The Effect of Colored and White Light on Growth and Phycobiliproteins, Chlorophyll and Carotenoids Content of the Marine Cyanobacteria Phormidium sp. and Cyanothece sp. in Batch Cultures. *Life*, 12(6):837, June 2022. Number: 6 Publisher: Multidisciplinary Digital Publishing Institute.

[91] Fernando Pagels, Vitor Vasconcelos, and Ana Catarina Guedes. Carotenoids from Cyanobacteria: Biotechnological Potential and Optimization Strategies. *Biomolecules*, 11(5):735, May 2021. Number: 5 Publisher: Multidisciplinary Digital Publishing Institute.

[92] Ming Su, Jiao Fang, Zeyu Jia, Yuliang Su, Yiping Zhu, Bin Wu, John C. Little, Jianwei Yu, and Min Yang. Biosynthesis of 2-methylisoborneol is regulated by chromatic acclimation of *Pseudanabaena*. *Environmental Research*, 221:115260, March 2023.

[93] Julia Jodlbauer, Thomas Rohr, Oliver Spadiut, Marko D. Mihovilovic, and Florian Rudroff. Biocatalysis in green and blue: Cyanobacteria, 9 2021.

[94] Jianhua Fan, Yinghui Zhang, Ping Wu, Xiaoyan Zhang, and Yunpeng Bai. Enhancing cofactor regeneration of cyanobacteria for the light-powered synthesis of chiral alcohols. *Bioorganic Chemistry*, 118, 1 2022.

[95] Jie Cheng, Chaobo Zhang, Kaidian Zhang, Jiashun Li, Yuyong Hou, Jiachao Xin, Yang Sun, Chengshuai Xu, and Wei Xu. Cyanobacteria-mediated light-driven biotransformation: The current status and perspectives, 11 2023.

[96] Kiyan Shabestary, Hugo Pineda Hernández, Rui Miao, Emil Ljungqvist, Olivia Hallman, Emil Sporre, Filipe Branco dos Santos, and Elton P Hudson. Cycling between growth and production phases increases cyanobacteria bioproduction of lactate. *Metabolic Engineering*, 68:131–141, 11 2021.

[97] Lisa B. Wiltbank and David M. Kehoe. Diverse light responses of cyanobacteria mediated by phytochrome superfamily photoreceptors. *Nature Reviews Microbiology*, 17(1):37–50, January 2019.

[98] Hiroki Hoshino, Keita Miyake, and Rei Narikawa. Chapter 15 - Cyanobacterial photoreceptors and their applications. In Hakuto Kageyama and Rungaroon Waditee-Sirisattha, editors, *Cyanobacterial Physiology*, pages 201–210. Academic Press, January 2022.

[99] Masumi Hasegawa, Toshiaki Hosaka, Keiichi Kojima, Yosuke Nishimura, Yu Nakajima, Tomomi Kimura-Someya, Mikako Shirouzu, Yuki Sudo, and Susumu Yoshizawa. A unique clade of light-driven proton-pumping rhodopsins evolved in the cyanobacterial lineage. *Scientific Reports*, 10(1):16752, October 2020.

[100] R. Astashkin, K. Kovalev, S. Bukhdruker, S. Vaganova, A. Kuzmin, A. Alekseev, T. Balandin, D. Zabelskii, I. Gushchin, A. Royant, D. Volkov, G. Bourenkov, E. Koonin, M. Engelhard, E. Bamberg, and V. Gordeliy. Structural insights into light-driven anion pumping in cyanobacteria. *Nature Communications*, 13(1):6460, October 2022.

[101] Melissa Cano, Steven C Holland, Juliana Artier, Rob L Burnap, Maria Ghirardi, John A Morgan, and Jianping Yu. Glycogen Synthesis and Metabolite Overflow Contribute to Energy Balancing in Cyanobacteria. *Cell Reports*, 23(3):667–672, 4 2018.

[102] Liat Adler, Aranzazú Díaz-Ramos, Yuwei Mao, Krzysztof Robin Pukacz, Chenyi Fei, and Alistair J McCormick. New horizons for building pyrenoid-based CO2-concentrating mechanisms in plants to improve yields. *Plant Physiology*, 190(3):1609–1627, 10 2022.

[103] Amel Latifi, Marion Ruiz, and Cheng-Cai Zhang. Oxidative stress in cyanobacteria. *FEMS Microbiology Reviews*, 33(2):258–278, March 2009.

[104] Hui Lyu and Dušan Lazár. Analyzing the effect of ion binding to the membrane-surface on regulating the light-induced transthylakoid electric potential ($\Delta\Psi$m). *Frontiers in Plant Science*, 13, 7 2022.

[105] Laura Roxana Stingaciu, Hugh O'Neill, Michelle Liberton, Volker S. Urban, Himadri B. Pakrasi, and Michael Ohl. Revealing the Dynamics of Thylakoid Membranes in Living Cyanobacterial Cells. *Scientific Reports*, 6, 1 2016.

[106] Markus Janasch, Johannes Asplund-Samuelsson, Ralf Steuer, and Elton P Hudson. Kinetic modeling of the Calvin cycle identifies flux control and stable metabolomes in Synechocystis carbon fixation. *Journal of Experimental Botany*, 70(3):973–983, 2019.

[107] Marvin van Aalst, Oliver Ebenhöh, and Anna Matuszyńska. Constructing and analysing dynamic models with modelbase v1.2.3: a software update. *BMC Bioinformatics*, 22(1):1–15, 4 2021.

[108] Shigeharu Kihara, Daniel A. Hartzler, and Sergei Savikhin. Oxygen concentration inside a functioning photosynthetic cell. *Biophysical Journal*, 106(9):1882–1889, may 2014.

[109] Ulrich Schreiber. Redox changes of ferredoxin, P700, and plastocyanin measured simultaneously in intact leaves. *Photosynthesis Research*, 134(3):343–360, dec 2017.

[110] Kenya Tanaka, Ginga Shimakawa, Hiro Tabata, Shoko Kusama, Chikahiro Miyake, and Shuji Nakanishi. Quantification of NAD(P)H in cyanobacterial cells by a phenol extraction method. *Photosynthesis Research*, 148(1):57, may 2021.

[111] Sofia Doello, Alexander Klotz, Alexander Makowka, Kirstin Gutekunst, and Karl Forchhammer. A Specific Glycogen Mobilization Strategy Enables Rapid Awakening of Dormant Cyanobacteria from Chlorosis. *Plant Physiology*, 177(2):594–603, jun 2018.

[112] Jan Huege, Jan Goetze, Doreen Schwarz, Hermann Bauwe, Martin Hagemann, and Joachim Kopka. Modulation of the Major Paths of Carbon in Photorespiratory Mutants of Synechocystis. *PLOS ONE*, 6(1):e16278, 2011.

[113] Yuan-Hui Li and Tien-Fung Tsui. The solubility of CO 2 in water and sea water . *Journal of Geophysical Research*, 76(18):4203–4207, 1971.

[114] Yu Tsukamoto, Yuriko Fukushima, Satoshi Hara, and Toru Hisabori. Redox Control of the Activity of Phosphoglycerate Kinase in Synechocystis sp. PCC6803. *Plant and Cell Physiology*, 54(4):484–491, apr 2013.

[115] Laure Michelet, Mirko Zaffagnini, Samuel Morisse, Francesca Sparla, María Esther Pérez-Pérez, Francesco Francia, Antoine Danon, Christophe H. Marchand, Simona Fermani, Paolo Trost, and Stéphane D. Lemaire. Redox regulation of the Calvin–Benson cycle: something old, something new. *Frontiers in Plant Science*, 4:470, November 2013.

[116] Adjélé Wilson, Claire Punginelli, Andrew Gall, Cosimo Bonetti, Maxime Alexandre, Jean Marc Routaboul, Cheryl A Kerfeld, Rienk Van Grondelle, Bruno Robert, John T M Kennis, and Diana Kirilovsky. A photoactive carotenoid protein acting as light intensity sensor. *Proceedings of the National Academy of Sciences*, 105(33):12075–12080, 8 2008.

[117] Martin Hagemann, Shanshan Song, and Eva-Maria Eva-Maria Brouwer. Inorganic Carbon Assimilation in Cyanobacteria: Mechanisms, Regulation, and Engineering. *Cyanobacteria Biotechnology*, pages 1–31, may 2021.

[118] Maximilian König, Jan Vaes, Elias Klemm, and Deepak Pant. Solvents and Supporting Electrolytes in the Electrocatalytic Reduction of CO2. *iScience*, 19:135–160, 9 2019.

[119] Francisco Javier Mojica Prieto and Frank J. Millero. The values of pK1 + pK2 for the dissociation of carbonic acid in seawater. *Geochimica et Cosmochimica Acta*, 66(14):2529–2540, jul 2002.

[120] Joris J. Benschop, Murray R. Badger, and G. Dean Price. Characterisation of CO2 and HCO3- uptake in the cyanobacterium Synechocystis sp. PCC6803. *Photosynthesis Research*, 77(2):117–126, August 2003.

[121] Gwenaëlle Moal and Bernard Lagoutte. Photo-induced electron transfer from photosystem I to NADP+: Characterization and tentative simulation of the in vivo environment. *Biochimica et Biophysica Acta (BBA) - Bioenergetics*, 1817(9):1635–1645, sep 2012.

[122] Nir Keren, Rajeev Aurora, and Himadri B. Pakrasi. Critical Roles of Bacterioferritins in Iron Storage and Proliferation of Cyanobacteria. *Plant Physiology*, 135(3):1666, 2004.

[123] Allison M.L. Van De Meene, William P. Sharp, Jennifer H. McDaniel, Heiner Friedrich, Wim F.J. Vermaas, and Robert W. Roberson. Gross morphological changes in thylakoid membrane structure are associated with photosystem I deletion in Synechocystis sp. PCC 6803. *Biochimica et Biophysica Acta (BBA) - Biomembranes*, 1818(5):1427–1434, may 2012.

[124] Denys Pogoryelov, Christian Reichen, Adriana L. Klyszejko, René Brunisholz, Daniel J. Muller, Peter Dimroth, and Thomas Meier. The oligomeric state of c rings from cyanobacterial F-ATP synthases varies from 13 to 15. *Journal of bacteriology*, 189(16):5895–5902, aug 2007.

[125] Andrew S. Richardson. *2019 NRL Plasma Formulary*. U.S. Naval Research Laboratory, 2019.

[126] Michael E. Wieser. Atomic weights of the elements 2005 (IUPAC Technical Report). *Pure and Applied Chemistry*, 78(11):2051–2066, jan 2006.

[127] Jocelyn Kauny and Pierre Sétif. NADPH fluorescence in the cyanobacterium Synechocystis sp. PCC 6803: A versatile probe for in vivo measurements of rates, yields and pools. *Biochimica et Biophysica Acta (BBA) - Bioenergetics*, 1837(6):792–801, jun 2014.

[128] Paul G. Falkowski and John A. Raven. *Aquatic Photosynthesis*. Princeton University Press, jan 2007.

[129] Gábor Bernát, Nadine Waschewski, and Matthias Rögner. Towards efficient hydrogen production: The impact of antenna size and external factors on electron transport dynamics in Synechocystis PCC 6803. *Photosynthesis Research*, 99(3):205–216, 2009.

[130] Pierre Sétif, Ginga Shimakawa, Anja Krieger-Liszkay, and Chikahiro Miyake. Identification of the electron donor to flavodiiron proteins in Synechocystis sp. PCC 6803 by in vivo spectroscopy. *Biochimica et Biophysica Acta (BBA) - Bioenergetics*, 1861(10):148256, oct 2020.

[131] Maria Ermakova, Tuomas Huokko, Pierre Richaud, Luca Bersanini, Christopher J. Howe, David J. Lea-Smith, Gilles Peltier, and Yagut Allahverdiyeva. Distinguishing the Roles of Thylakoid Respiratory Terminal Oxidases in the Cyanobacterium Synechocystis sp. PCC 6803. *Plant Physiology*, 171(2):1307–1319, jun 2016.

[132] Lijin Tian, Ivo H. M. van Stokkum, Rob B. M. Koehorst, Aniek Jongerius, Diana Kirilovsky, and Herbert van Amerongen. Site, Rate, and Mechanism of Photoprotective Quenching in Cyanobacteria. *Journal of the American Chemical Society*, 133(45):18304–18311, nov 2011.

[133] Tomáš Zavřel, Petra Očenášová, and Jan Červený. Phenotypic characterization of Synechocystis sp. PCC 6803 substrains reveals differences in sensitivity to abiotic stress. *PLoS ONE*, 12(12), dec 2017.

[134] Yonatan Savir, Elad Noor, Ron Milo, and Tsvi Tlusty. Cross-species analysis traces adaptation of Rubisco toward optimality in a low-dimensional landscape. *Proceedings of the National Academy of Sciences*, 107(8):3475–3480, feb 2010.

[135] Akira Wadano, Keisuke Nishikawa, Tomohiro Hirahashi, Ryohei Satoh, and Toshio Iwaki. Reaction mechanism of phosphoribulokinase from a cyanobacterium, Synechococcus PCC7942. *Photosynthesis Research*, 56(1):27–33, 1998.

[136] Olga Koksharova, Milada Schubert, Sergey Shestakov, and Rüdiger Cerff. Genetic and biochemical evidence for distinct key functions of two highly divergent GAPDH genes in catabolic and anabolic carbon flow of the cyanobacterium Synechocystis sp. PCC 6803. *Plant Molecular Biology*, 36:183, 1998.

[137] Taras K. Antal, Ilya B. Kovalenko, Andrew B. Rubin, and Esa Tyystjärvi. Photosynthesis-related quantities for education and modeling. *Photosynthesis Research*, 117(1-3):1–30, November 2013.